AMERICAN SOCIETY FOR MICROBIOLOGY | mBio®

RESEARCH ARTICLE
Molecular Biology and Physiology

Lipoprotein *N*-Acylation in *Staphylococcus aureus* Is Catalyzed by a Two-Component Acyl Transferase System

John H. Gardiner IV,[a] Gloria Komazin,[b] Miki Matsuo,[c] Kaitlin Cole,[b] Friedrich Götz,[c] Timothy C. Meredith[a,b]

[a]The Huck Institutes of the Life Sciences, The Pennsylvania State University, University Park, Pennsylvania, USA
[b]Department of Biochemistry and Molecular Biology, The Pennsylvania State University, University Park, Pennsylvania, USA
[c]Microbial Genetics, Interfaculty Institute of Microbiology and Infection Medicine Tübingen, University of Tübingen, Tübingen, Germany

ABSTRACT Bacterial lipoproteins (Lpps) are a class of membrane-associated proteins universally distributed among all bacteria. A characteristic N-terminal cysteine residue that is variably acylated anchors C-terminal globular domains to the extracellular surface, where they serve numerous roles, including in the capture and transport of essential nutrients. Lpps are also ligands for the Toll-like receptor 2 (TLR2) family, a key component of the innate immune system tasked with bacterial recognition. While Lpp function is conserved in all prokaryotes, structural heterogeneity in the N-terminal acylation state is widespread among *Firmicutes* and can differ between otherwise closely related species. In this study, we identify a novel two-gene system that directs the synthesis of *N*-acylated Lpps in the commensal and opportunistic pathogen subset of staphylococci. The two genes, which we have named the lipoprotein *N*-acylation transferase system (Lns), bear no resemblance to previously characterized N-terminal Lpp tailoring enzymes. LnsA (SAOUHSC_00822) is an NlpC/P60 superfamily enzyme, whereas LnsB (SAOHSC_02761) has remote homology to the CAAX protease and bacteriocin-processing enzyme (CPBP) family. Both LnsA and LnsB are together necessary and alone sufficient for *N*-acylation in *Staphylococcus aureus* and convert the Lpp chemotype from diacyl to triacyl when heterologously expressed in *Listeria monocytogenes*. Acquisition of *lnsAB* decreases TLR2-mediated detection of *S. aureus* by nearly 10-fold and shifts the activated TLR2 complex from TLR2/6 to TLR2/1. LnsAB thus has a dual role in attenuating TLR2 signaling in addition to a broader role in bacterial cell envelope physiology.

IMPORTANCE Although it has long been known that *S. aureus* forms triacylated Lpps, a lack of homologs to known *N*-acylation genes found in Gram-negative bacteria has until now precluded identification of the genes responsible for this Lpp modification. Here, we demonstrate N-terminal Lpp acylation and chemotype conversion to the tri-acylated state is directed by a unique acyl transferase system encoded by two noncontiguous staphylococci genes (*lnsAB*). Since triacylated Lpps stimulate TLR2 more weakly than their diacylated counterparts, Lpp *N*-acylation is an important TLR2 immunoevasion factor for determining tolerance or nontolerance in niches such as in the skin microbiota. The discovery of the LnsAB system expands the known diversity of Lpp biosynthesis pathways and acyl transfer biochemistry in bacteria, advances our understanding of Lpp structural heterogeneity, and helps differentiate commensal and noncommensal microbiota.

KEYWORDS *Staphylococcus*, *Staphylococcus aureus*, TLR2, acyl transferases, immune response, lipoproteins, Toll-like receptors

Bacterial lipoproteins (Lpps) are ubiquitous components of bacterial cell membranes containing a characteristic lipid-modified N-terminal cysteine residue that anchors C-terminal globular protein domains to the cell surface (1–3). Lpps comprise, on

Citation Gardiner JH, IV, Komazin G, Matsuo M, Cole K, Götz F, Meredith TC. 2020. Lipoprotein *N*-acylation in *Staphylococcus aureus* is catalyzed by a two-component acyl transferase system. mBio 11:e01619-20. https://doi.org/10.1128/mBio.01619-20.

Invited Editor Marcin Grabowicz, Emory University School of Medicine

Editor M. Stephen Trent, University of Georgia

Address correspondence to Timothy C. Meredith, txm50@psu.edu.

Received 17 June 2020
Accepted 26 June 2020
Published 28 July 2020

average, ~2.7% of all prokaryotic open reading frames and perform a wide variety of cellular functions occurring at the interface of the extracellular bacterial surface with the environment (4). In the Gram-positive opportunistic pathogen *Staphylococcus aureus*, there are approximately 70 total Lpp-encoding genes (5, 6), of which a highly conserved 60-member subset is present across genetically diverse lineages. While cellular roles for much of the lipoproteome remain uncharacterized, many Lpps are involved in the uptake of essential nutrients, as well as in maintaining general bacterial fitness and virulence. Iron capture and transport is a particularly critical factor in establishing infections, and *S. aureus* has devoted multiple Lpps for this purpose (7, 8). The accessory *lpp* gene subset is more limited, being scattered throughout the core genome and within pathogenicity-associated islands in certain virulent *S. aureus* isolates. Tandem-type Lpps (also called lipoprotein-like [Lpl] or DUF576 proteins), for instance, are an abundant paralogous gene family present in multicopy clusters in discrete loci throughout the genome (5). It has been suggested that Lpl diversity is the result of recombination-driven antigenic variation (9) and that Lpl promotes host cell invasion by binding to Hsp90 (10).

The integral roles of Lpps in bacterial physiology and fitness, in combination with their abundance, extracellular locale, conserved structure, and widespread distribution among all bacteria, make them a key focal point for recognition by the innate immune system (11). A unique thioether-linked diacylglycerol moiety attached to the N-terminal cysteine of Lpp is recognized by heterodimeric Toll-like receptor 2 (TLR2) complexes, a group of integral membrane proteins expressed by macrophages and other immune-related cells (12). The TLR2 proteins (TLR2/TLR1/TLR6) are pattern recognition receptors with leucine-rich repeat ectodomains that bind external Lpp ligand, leading to the dimerization of intracellular Toll–interleukin-1 receptor (TIR) homology domains. TIR domain dimerization activates the MyD88-dependent intracellular signaling pathway, inducing translocation of nuclear factor-κB (NF-κB) and proinflammatory cytokine secretion to help clear the bacterial infection (13–15). A thioether-linked acylated glycerol substituent is common to all bacterial Lpp chemotypes and is the core ligand recognition feature of TLR2. The state of the N-terminal cysteine dictates the TLR2 dimerization partner (TLR1 or TLR6). In most Gram-negative bacteria, the N terminus is modified to form triacylated Lpp (TA-Lpp) (2). The amide-linked acyl chain is critical for substrate recognition and efficient trafficking to the outer membrane by the Lpp transport system (Lol) (16). In the TLR2/1 heterodimer, TLR2 binds the diacylglycerol region, while the hydrophobic pocket in TLR1 accommodates the *N*-acyl chain (17). Many Gram-positive bacteria, which lack an outer membrane and do not need Lol-mediated transport, retain diacylated Lpps with free α-amino termini (DA-Lpps). DA-Lpps are recognized by TLR2/TLR6 heterodimers, with TLR2 binding diacylglycerol and TLR6 interacting with the α-amino group (18).

While it was previously thought that DA-Lpp from Gram-positive and TA-Lpp from Gram-negative bacteria represented all bacterial Lpp chemotypes, novel structures have since been discovered. In a survey of the Gram-positive phylum *Firmicutes*, *N*-acetyl, *N*-peptidyl, lyso-Lpp (lyso-form lipoprotein), and *N*-acylated TA-Lpp similar in structure to Gram-negative bacteria have now been characterized (19). Clearly, N-terminal modification has a purpose beyond Lpp trafficking to the outer membrane. We recently identified the lipoprotein intramolecular transferase (Lit) enzyme in *Enterococcus faecalis* that catalyzes the internal migration of the *sn*-2 acyl chain of the di-acylglycerol moiety in DA-Lpp substrate to the *N* terminus (20). The resulting lyso-Lpp chemotype still retains two total acyl chains but becomes a much weaker TLR2/6 ligand, and almost undetectable by TLR2/1 activity despite being *N*-acylated (21). The TLR2/1/6 response to lyso-Lpp decreases 100- to 1,000-fold when challenged with either model lipopeptides or heat-killed whole cells as ligands. In comparison to the DA-Lpp-producing type strain of *Listeria monocytogenes*, much higher relative bacterial cell concentrations of *E. faecalis* are needed to trigger a TLR2 response (21). Lpp chemotype conversion within a species can also attenuate TLR2 activity. Certain *L. monocytogenes* environmental isolates have acquired a plasmid-borne, copper-

inducible *lit2* paralog that induces a weaker TLR2 response when grown in copper-supplemented media (21). Among staphylococci, *Staphylococcus carnosus* forms *N*-acetylated Lpps and induces 10-fold higher levels of the proinflammatory IL-6 cytokine than does *S. aureus* with TA-Lpp (22, 23). Differences in immunostimulation among Lpp chemotypes thus helps to define the potential for virulence, as well as to facilitate the niche-specific adaptation of commensal bacteria from closely related noncommensal isolates (23).

Many of the enzymes directing Lpp N-terminal tailoring reactions, which in turn can modulate host TLR2 responses, remain to be discovered. Of particular note, *S. aureus* synthesizes TA-Lpp despite lacking an apparent ortholog to the *N*-acyl transferase (Lnt) used in Gram-negative bacteria (24–26). Schneewind and coworkers first reported on a base-stable Lpp acyl group, suggesting the presence of an amide-linked *N*-acyl chain (27). Analysis by mass spectrometry subsequently followed and provided direct structural evidence that unequivocally confirmed the TA-Lpp chemotype in *S. aureus* (28, 29). Here, we report the identification of two previously uncharacterized genes (SAOUHSC_00822 and SAOUHSC_02761) in *S. aureus* required for this Lpp *N*-acylation using a TLR2/1-specific reporter assay to screen a random transposon library. We named this novel two-component Lpp tailoring machinery the Lipoprotein *N*-acyl transferase system (LnsA and LnsB). Neither LnsA or LnsB share any sequence similarity to Lnt or Lit, and both are only present in *Staphylococcus* species thus far known to make TA-Lpp. We show that loss of either gene in *S. aureus* converts TA-Lpp to DA-Lpp and that both genes are absolutely required and together sufficient to convert DA-Lpp to TA-Lpp in the *L. monocytogenes*. In either host, TLR2 challenge with DA-Lpp-producing strains induced a more potent response relative to isogenic TA-Lpp counterparts. Deletion of either *lnsA* or *lnsB* increased interleukin-8 (IL-8) secretion nearly 10-fold, indicating LnsAB are important determinants acquired by commensal and opportunistic staphylococci pathogens to evade TLR2 immune surveillance. The discovery of the presumptive two-component LnsAB complex expands the known diversity of Lpp tailoring reactions in bacteria.

RESULTS

Transposon library screen for diminished TLR2/1 signaling. We initially hypothesized that a single integral membrane protein in *Staphylococcus aureus* performs an analogous function to Lnt from *Escherichia coli*. Our selection strategy using growth rescue of an *E. coli* Lnt-depletion strain, however, that had successfully identified *lit* from *Enterococcus faecalis* and *Bacillus cereus* genomic DNA libraries (20) repeatedly failed when using *S. aureus* genomic DNA as the input library (data not shown). We thus turned to an indirect phenotypic screen to monitor loss of TLR2/1 signal, which has significantly higher affinity for TA-Lpp than DA-Lpp ligand, paired with a TLR2/6 specific activity counterscreen to eliminate candidates expressing either less total Lpp or that grew to a lower final biomass. Colonies from a high-coverage *S. aureus* mariner transposon (Tn) library built in the model lab strain NCTC8325 were used in the TLR2 reporter assays (30). We screened ~4,000 Tn mutants, and identified two unique Tn insertions in proximity to the unidentified open reading frame SAOUHSC_02761 (see Fig. S1 in the supplemental material). SAOUHSC_02761 is predicted to be a polytopic integral membrane protein by TMHMM2.0 (31), and has no sequence similarity with functionally annotated conserved domains. Remote protein homology with CAAX protein proteases (32) can be detected using HHPred, an algorithm that considers structure, as well as sequencing, to identify distant homology (33). The first Tn mutant (Tn 16C2) inserted 18 bp upstream from the SAOUHSC_02761 start codon, while the second (Tn 32F1) disrupted the coding region (amino acid 114 of a 249-amino-acid SAOUHSC_02761 ORF) (Fig. S1A). Northern blotting using an antisense SAOUHSC_02716 N-terminal probe confirmed a monocistronic transcript, that Tn 16C2 prevents readthrough expression, and that 32F1 expresses a longer transcript that is predicted to be frameshifted (Fig. S1B). Both Tn mutants

had markedly diminished TLR2/1-specific stimulating activity comparable to disruption of the other known Lpp biosynthetic pathway enzymes, lipoprotein diacylglycerol transferase (Lgt) and lipoprotein signal peptidase II (Lsp) (Fig. S1C). Lgt links diacylglycerol through a thioether bond using a neighboring phospholipid to make preapolipoprotein on the extracellular membrane surface (34, 35), which Lsp then cleaves to liberate the free α-amino cysteine terminus and complete DA-Lpp formation (36). Unlike Tn insertion in *lgt* and *lsp*, both Tn 16C2 and 32F1 mutants retained TLR2/6 activity at least as active as wild type (Fig. S1D). This is consistent with a common loss of SAOUHSC_02716 function genotype for both Tn mutants.

Although the immunoassay data implicated SAOUHSC_02761 in TA-Lpp formation, introducing SAOUHSC_02761 into an *E. coli* Lnt depletion strain failed to rescue growth (data not shown). We presumed an issue with heterologous expression or the available fatty acid donor pool in *E. coli*, so we repeated the TLR2 immunoassay using *L. monocytogenes*. Both *S. aureus* and *L. monocytogenes* have saturated branched-chain fatty acids (37, 38), utilize acyl-phosphate donors in glycerophospholipid biosynthesis (39, 40), and in general share much cell envelope physiology. However, introduction of SAOUHSC_02761 once again failed to induce phenotypic conversion (see below), indicating SAOUHSC_02761 may be required for TA-Lpp formation but not alone sufficient. We took advantage of the prearrayed Nebraska Transposon Mutant Library (NTML) in the *S. aureus* JE2 USA300 clinical isolate to repeat the TLR2/1 specific immunoactivity screen (Fig. 1A). We identified six Tn gene disruption mutants with decreased activity, including in SAUSA300_2405 [Tn NE407(Tn*2405*) or SAOUHSC_02761 in strain NCTC8325], *lgt*, and *lsp*. The only Tn library mutant besides SAUSA300_2405 that retained TLR2/6 activity while growing to a normal final biomass had an insertion in the uncharacterized open reading frame SAUSA300_0780 [Tn NE536(Tn*0780*) or SAOUHSC_00822 in strain NCTC8325]. The SAUSA300_0780/SAOUHSC_00822 gene encodes a 189-amino-acid protein containing a domain with very weak similarity to the NlpC/P60 endopeptidase superfamily (41) and is predicted by SignalP v5.0 to contain a signal peptide for extracellular transport (42). As with SAUSA300_2405/SAOUHSC_02761, this gene is expressed under standard culture conditions but is part of a polycistronic operon as judged by transcript length (Fig. S1B). Expression levels of SAUSA300_0780/SAOUHSC_00822 were constant and not reliant on SAUSA300_2405/SAOUHSC_02761 function. Tn insertion in either SAUSA300_0780 or SAUSA300_2405 in *S. aureus* USA300 JE2 decreased TLR2/1 activation by $>$50-fold compared to the wild type (Fig. 1B).

To confirm we had identified all candidate genes required for synthesis of a TLR2/1-active Lpp chemotype, we heterologously expressed both SAOUHSC_00822 and SAOUHSC_0276 in *L. monocytogenes*. *L. monocytogenes* normally makes DA-Lpp, so introduction of both candidate genes from *S. aureus* should impart TLR2/1 activity. While either gene alone did not produce TLR2/1 signal, the expression of both genes with a constitutive promoter markedly enhanced the TLR2/1 response (Fig. 1C). Although other genes (such as those providing the acyl donor) may be required for Lpp chemotype conversion, these genes are evidently not specific to *S. aureus*.

Deletion of either SAOUHSC_00822 or SAOUHSC_02761 decreases detection by TLR2/1 while enhancing TLR2/6 activity. To determine whether the decrease in TLR2/1 signal was solely due to Tn disruption and whether the two mutations are additive, we constructed targeted in-frame deletions of both genes in the *S. aureus* NCTC8325 background and measured TLR2/1 and TLR2/6 activity (Fig. 2). All deletion strains grew at rates statistically identical to the parent wild-type strain. Dilution series of heat-killed bacterial culture extracts were applied to TLR2/1-expressing reporter cells, and transcriptional activation of NF-κB was measured. Deletion of either or both genes in tandem decreased the signal equivalently, which could be restored to near-wild-type levels by plasmid back-complementation (Fig. 2A). With TLR2/6 assays, activity increased to the same extent in the single and double gene deletion constructs (Fig. 2B). The opposing TLR2 response indicates SAOUHSC_00822 and SAOUHSC_02761 are mutually required to swap TLR2 receptor ligand specificity. Since any combination of

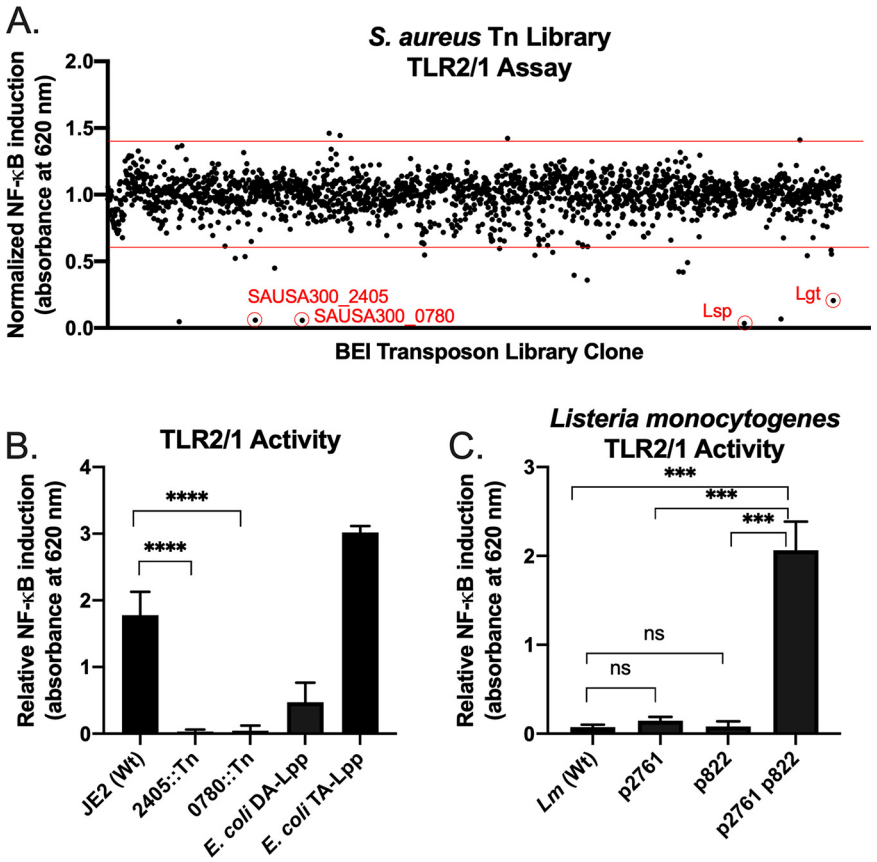

FIG 1 TLR2 activity of *S. aureus* USA300 Tn mutants. (A) Heat-killed extracts were prepared from all 1920 Tn mutants in the NTML prearrayed library. Induction of NF-κB was measured colorimetrically through secretion of alkaline phosphatase. Raw absorbance values were normalized to the average absorbance across the entire library. Among the Tn mutants demonstrating changes in absorbance exceeding the norm by more than three standard deviations (red horizontal lines), four hits were robust and could be consistently replicated. Two were in known enzymes involved in Lpp biosynthesis (*lgt*::Tn and *lsp*::Tn), while two were in uncharacterized open reading frames [NE536 (SAUSA300_0780::Tn) and NE407 (SAUSA300_2405::Tn)]. (B) The TLR2/1 specific activity was measured for both new genetic determinants (SAUSA300_0780::Tn and SAUSA300_2405::Tn) and compared to wild type (JE2) and Lpp control chemotypes (triacylated [TA-Lpp] and diacylated [DA-Lpp]) from *E. coli* donor strains. Error bars represent the standard deviation results of at least three replicates. (C) The TLR2/1 specific activity was measured from heat-killed extracts from wild-type *L. monocytogenes* (expressing DA-Lpp) and isogenic strains expressing SAOUHSC_02761 (same as SAUSA300_2405, p2761), SAOUHSC_00822 (same as SAUSA300_0780, p822), or both genes together (p2761, p822). Statistical significances were calculated by using Student *t* tests (*, $P < 0.05$; **, $P < 0.01$; ***, $P < 0.001$; ****, $P < 0.0001$; ns, not significant).

gene deletion alleles elicited equal changes in the TLR2 response, SAOUHSC_00822 and SAOUHSC_02761 are therefore codependent and not separate components of redundant Lpp *N*-acylation pathways.

SAOUHSC_00822 and SAOUHSC_02761 alter the Lpp profile in *S. aureus*. To correlate changes in TLR2 immunoassay data (Fig. 2) with Lpp structure, we introduced a plasmid encoding a fragment of the *S. aureus* SitC Lpp with a C-terminal strep tag probe under the control of the constitutive promoter P_{tuf} (Fig. 3A). The probe contained an N-terminal signal peptide for export, a lipobox for recognition by Lgt and Lsp for maturation, and the first 9 amino acids of SitC following the N-terminal cysteine linked to the strep tag epitope. The short probe length allowed separation of Lpp chemotypes with small mass differences by SDS-PAGE, including those due to total number of acyl chains. All *S. aureus* Lpp extracts produced a single homogenous band (Fig. 3B). In comparison to the wild type, the ΔSAOUHSC_00822 and ΔSAOUHSC_02761 constructs produced faster-migrating Lpp chemotypes that could be reverted back to wild type by plasmid

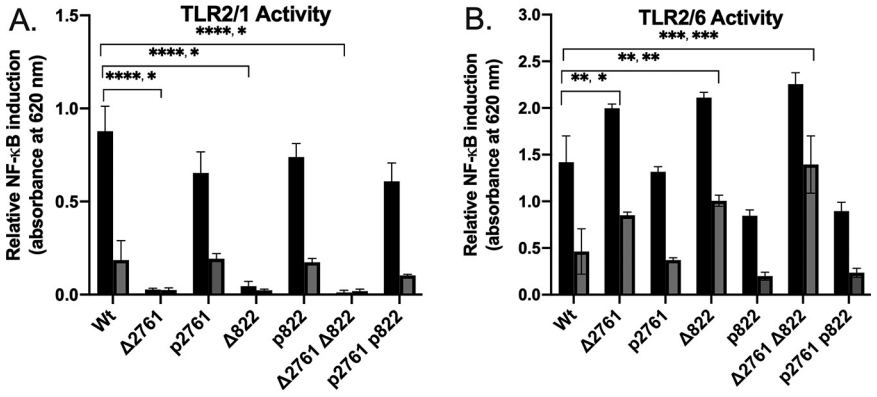

FIG 2 TLR2 activity of gene deletion mutants in *S. aureus* NCTC8325. TLR2 activation through either TLR2/1 or TLR2/6 was measured by NF-κB induction. (A) TLR2/1 receptor activity was measured in parent strain *S. aureus* TM226 (Wt), in single gene deletion mutants (ΔSAOUHSC_02761 [Δ2761], Δ2761 with plasmid back-complementation [p2761], ΔSAOUHSC_00822 [Δ822], and Δ822 with plasmid back-complementation [p822]), and in double gene deletion mutants (Δ2761Δ822, Δ2761Δ822 with plasmid back-complementation [p2761, p822]). Heat-killed bacterial extracts were applied either as concentrated (black) or 5-fold diluted (gray) aliquots. (B) TLR2/6 receptor activity using the same extracts as in panel A, except that concentrated (black) or 10-fold-diluted (gray) aliquots were used. Error bars in both panels represent standard deviation results of at least three experimental replicates. Statistical significances (listed for black and gray bars) were calculated by using Student *t* tests (*, $P < 0.05$; **, $P < 0.01$; ***, $P < 0.001$; ****, $P < 0.0001$).

back-complementation. Deletion of both genes (ΔSAOUHSC_00822 ΔSAOUHSC_02761) did not further change the Lpp profile, confirming a mutually nonredundant role for these genes in Lpp modification. To determine whether one candidate gene was needed for transcription of the other, we repeated the assay using a constitutive promoter (P_{pen}). The extent of complementation was complete and identical to vectors with native promoters. The functional codependence of SAOUHSC_00822 and SAOUHSC_02761 is thus not based on transcriptional regulation in line with initial Northern blotting results (Fig. S1B).

SAOUHSC_00822 and SAOUHSC_02761 constitute a novel lipoprotein *N*-acylation system (LnsAB) directing TA-Lpp synthesis in *S. aureus*. To determine whether the mass shift observed by SDS-PAGE was indeed due to acylation state, native Lpps were extracted and analyzed by matrix-assisted laser desorption ionization–time of flight (MALDI-TOF) mass spectrometry (20, 43). The N-terminal lipopeptide spectrum from wild-type SitC yielded a characteristic series of ions differing by 14 U (-CH_2-), consistent with a highly heterogeneous population of lipopeptides varying in total acyl chain (Fig. 4). The majority of the total signal could be assigned to the TA-Lpp chemotype, with the C51 chemotype being the dominant ion ($M+H^+$ 1,353.06 U). Fragmentation

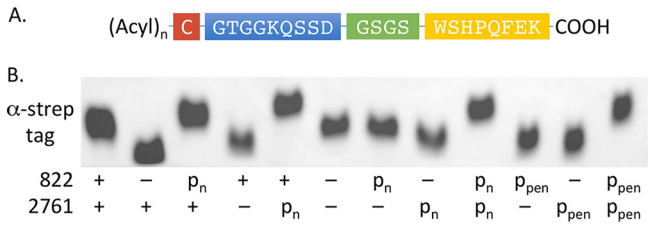

FIG 3 Immunoblot of SitC strep tag fragment expressed in *S. aureus* RN4220. (A) The SitC Lpp probe expressed by pLI50-sitC10AA is a 10-amino-acid SitC fragment with a C-terminal strep tag epitope and an *N*-acylated cysteine after being processed by Lgt and Lsp. Colors: red, N-terminal cysteine; blue, SitC fragment; green, linker; yellow, strep tag. (B) Total protein was extracted from lysostaphin treated cells and separated by SDS-PAGE before being transferred to a nitrocellulose membrane. The SitC probe was detected by immunoblotting with HRP α-strep tag conjugate. The SAOUHSC_00822 (822) and SAOUHSC_02761 genotypes (labeled 822 and 2761, respectively) are indicated, and results are representative of two separate experimental replicates. +, Present in chromosome; –, absent in chromosome; P_n, plasmid with native chromosomal promoter from *S. aureus*; P_{pen}, plasmid with constitutive promoter.

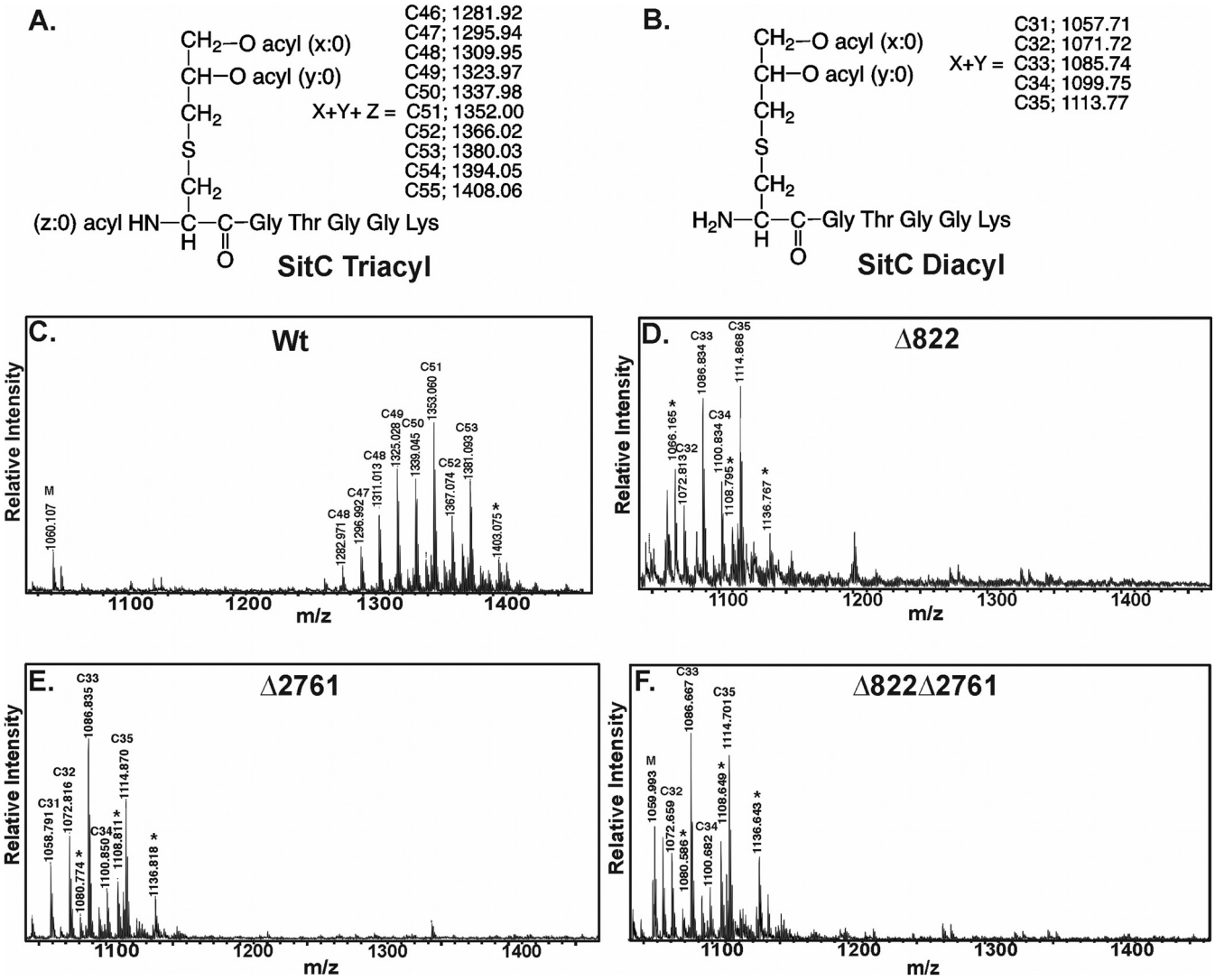

FIG 4 MALDI-TOF MS spectra of tryptic digest of *S. aureus* SitC Lpp. (A) The native structure of the N-terminal tryptic peptide of SitC Lpp in *S. aureus* is triacylated (TA-Lpp) and contains an amide-linked *N*-acyl chain. (B) Structure of the diacylated (DA-Lpp) N-terminal SitC tryptic lipopeptide. The calculated monoisotopic masses based on the sum total length of all acyl chains (C in carbon atoms) are indicated for TA-Lpp and DA-Lpp chemotypes. All acyl chains (ester-linked *sn*-1 *x*:0 and *sn*-2 *y*:0 plus amide-linked *z*:0) are assumed to be saturated. MALDI-TOF MS spectra of SitC N-terminal tryptic peptides in positive-ion mode were obtained from wild-type TM226 (Wt) (C), ΔSAOUHSC_00822 (D), ΔSAOUHSC_02761 (E), or the double-knockout ΔSAOUHSC_00822 ΔSAOUHSC_02761 strain (F). Sodiated adducts are represented by an asterisk (*). The α-CHCA matrix related peaks are labeled with an "M." The MS/MS fragment ion spectra used to assign the acylation state of the N terminus (Fig. S2), and the MS spectra of the corresponding plasmid back-complemented strains (Fig. S3) are provided in the supplemental material.

of the C51 sodiated parent ion adduct ($M+Na^+$ 1,375.06 U) produced a series of *N*-acyl dehydroalanyl signals separated by two methylene units (28 U), with $C_{18:0}$ being the most abundant *N*-acyl fatty acid substitution (Fig. S2A). In contrast, deletion of SAOUHSC_00822 or SAOUHSC_02761 yielded MS spectra containing lower molecular mass lipopeptide signals between 1,057 and 1,137 U (Fig. 4D and E). The most abundant signals were C33 and C35 Lpp chemotypes ($M+H^+$ 1086.7 U and 1114 u), nominally consistent with two acyl chains. Fragmentation of the C33 sodiated adduct ($M+H^+$ 1,108.7 U) confirmed the canonical DA-Lpp acyl chain distribution with a diacyl glycerol moiety and a free α-amino terminal cysteine (Fig. S2B). Deletion of both genes resulted in an identical MS profile with similar acyl chain composition to single gene deletion mutants (Fig. 4F). TA-Lpp synthesis could be restored in all constructs by plasmid back-complementation (Fig. S3). Analysis of a set of extracts from a different Lpp (SAOUHSC_02699) yielded identical results as with SitC (Fig. S4). The MALDI-TOF

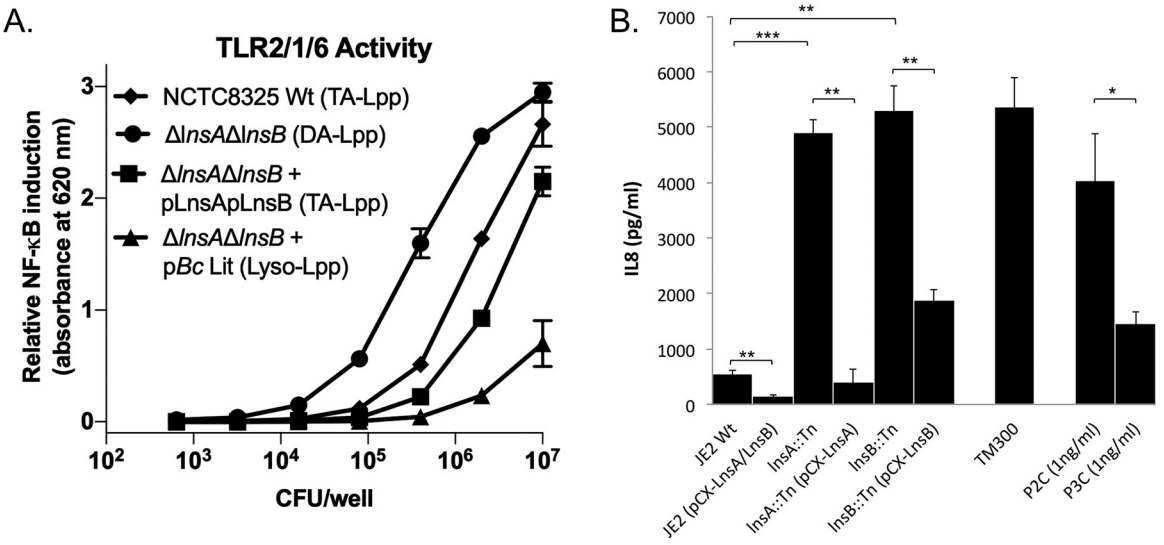

FIG 5 TLR2/1/6 activity and IL-8 induction in response to *S. aureus* Lpp chemotypes. (A) Relative NF-κB induction in HEK-Blue reporter cells (hTLR2/1/6) expressing both TLR2/1 and TLR2/6 receptor complexes were stimulated with either wild-type *S. aureus* NCTC8325, Δ*lnsA*Δ*lnsB*, Δ*lnsA*Δ*lnsB* + pLnsA pLnsB, or Δ*lnsA*Δ*lnsB* + p*Bc*Lit. The Lpp chemotype produced by each strain is indicated parenthetically. The data are from experiments conducted in triplicate and the error bars show standard deviation values. TA-Lpp, triacylated; DA-Lpp, diacylated; Lyso-Lpp, lyso-form. (B) IL-8 production (pg/ml) was measured after an 18-h stimulation of HEK-TLR2 cells with *S. aureus* USA300 wild-type JE2, JE2(pCX-LnsA/LnsB), Tn::*lnsA* (NE536), Tn::*lnsA*(pCX-LnsA), Tn::*lnsB* (NE407), Tn::*lnsB*(pCX-LnsB), and *S. carnosus* TM300. The MOI was 2. Tripalmitoylated (P3C) and dipalmitoylated (P2C) CSKKKK synthetic lipopeptides were used as controls for TLR2/1 and TLR2/6 activity, respectively. The experiments were conducted in triplicate and performed more than three times. The error bars indicate standard deviation values. Statistical significances were calculated by using Student *t* tests (*, $P < 0.05$; **, $P < 0.01$; ***, $P < 0.001$).

MS and MS-MS results confirm that SAOUHSC_00822 and SAOUHSC_02761 have nonredundant roles in TA-Lpp formation. We have thus annotated this novel Lipoprotein *N*-acylation System as LnsA (SAOUHSC_00822) and LnsB (SAOUHSC_02761).

N-terminal Lpp modification attenuates detection by TLR2/1/6. With the discovery of LnsAB, we could now directly compare the TLR2-stimulating potential of DA-Lpp, TA-Lpp, and lyso-Lpp chemotypes in the same *S. aureus* genetic background. Reporter cells expressing TLR2/1/6 (capable of binding both DA-Lpp and TA-Lpp ligand) were challenged with heat-killed bacterial cells, and the NF-κB transcriptional activation was measured (Fig. 5A). A clear hierarchy was observed in the bacterial cell count needed to reach half-maximal activation (EC_{50}). The EC_{50} of *S. aureus* expressing DA-Lpp was >100-fold lower in comparison to an isogenic lyso-Lpp forming strain carrying *lit* from *B. cereus*. The EC_{50} for wild-type *S. aureus* synthesizing TA-Lpp was intermediate, increasing the EC_{50} from DA-Lpp by 10-fold. Lpp chemotype potency for TLR2 activation is hence ordered (DA-Lpp > TA-Lpp > lyso-Lpp), demonstrating how *Firmicutes* Lpp N-terminal modification systems can alter TLR2 detection over more than 2 orders of magnitude.

In order to translate changes in the NF-κB transcriptional response into proinflammatory cytokine secretion, we repeated the assay using *lnsAB* Tn insertion mutants in the contemporary clinical isolate *S. aureus* USA300 [NE536(Tn*0780*)-LnsA and NE407(Tn*2405*)-LnsB initially identified in Fig. 2A]. If both *S. aureus* genes direct TA-Lpp formation, the immune-stimulating activity in *lnsAB* deletion mutants making only DA-Lpp should be significantly increased as well (Fig. 4). Immune stimulation was monitored by the production of IL-8. The wild-type JE2 parent produced only about 500 pg/ml, whereas in the two Tn mutants NE536(*lnsA*::Tn) and NE407(*lnsB*::Tn) the IL-8 production was ~10 times higher (Fig. 5B). When back-complemented in either NE536(pCX-LnsA) and NE407(pCX-LnsB), the IL-8 production was decreased. Conversely, when both genes were coexpressed in JE2 (pCX-LnsA/LnsB), IL-8 production was even further decreased, indicating high-level *N*-acyl transferase activity further shifted the Lpp chemotype population in favor of the weaker TA-Lpp TLR2 agonist. The

cytokine response is in complete agreement with the NF-κB transcriptional activation data. It has previously been shown that *N*-acetyl Lpp induces higher immune stimulation than TA-Lpp in *S. carnosus* (23), and direct comparison of *S. carnosus* to DA-Lpp-producing *S. aureus lnsA* or *lnsB* mutants demonstrated nearly equivalent activity. Thus, staphylococci forming *N*-acetyl or DA-Lpp are higher TLR2 activating agonists than their TA-LPP counterparts.

DISCUSSION

There is much naturally occurring structural diversity among Lpp chemotypes in *Firmicutes* (19). Unlike in Gram-negative bacteria, deletion of the core Lpp biosynthetic genes (Lgt and Lsp) in monoderm Gram-positive bacteria such as *S. aureus* induces a subtle phenotype in rich media (44), and a robust phenotype specifically attributable to the Lpp N-terminal acylation state has yet to be reported. We therefore utilized loss of TLR2/1 activation to identify bacterial mutants with changes in the Lpp N-terminal acylation state. We screened two separate *S. aureus* Tn insertion libraries and, surprisingly, identified two previously unknown genes necessary for TA-Lpp production that we have now named LnsA (SAOUHSC_00822) and LnsB (SAOUHSC_02761). Both *lnsAB* genes are absolutely required for TA-Lpp formation in *S. aureus* as determined by the Lpp SDS-PAGE profiles (Fig. 3) and MALDI-TOF mass spectrometry (Fig. 4; see also Fig. S4). LnsAB share no similarity with the two other known Lpp *N*-acylating enzymes in either primary amino acid sequence or mechanism. The apolipoprotein *N*-acyl transferase (Lnt) in Gram-negative bacteria utilizes the *sn*-1 acyl chain of phosphatidylethanolamine as an *N*-acyl chain donor (45), while Lit intramolecularly transfers the *sn*-2 acyl group of DA-Lpp to the α-amino terminus to form lyso-Lpp (46). The acyl chain source for LnsAB is currently unknown. While other genes may be needed to make the acyl donor, these genetic determinants are not unique to *S. aureus* since TLR2/1 agonist activity was conferred to *L. monocytogenes* by integrating just *lnsAB* into the genome (Fig. 1C).

TA-Lpp formation in *S. aureus* requires both LnsA and LnsB, but at present their respective roles in *N*-acylation are unknown. The top five proteins with homology to LnsA (YiiX [2IF6], 18% identity; BCE_A0238 [3KW0] [47], 14% identity; HRASLS-2/$PLA_{1/2}$-2 [4DPZ] [48], 13% identity; HRASLS-4/TIG3 [2LKT] [49], 14% identity; and HRASLS-3/H-REV107 [50], 15% identity) as predicted by HHPred (51) are all enzymes in the papain-like NlpC/P60 superfamily (41). The NlpC/P60 superfamily consists of four main families (P60-like, AcmB/LytN-like, YaeF/YiiX-like, and LRAT-like) that can be further grouped into the canonical CPNE (P60-like and AcmB/LytN-like) and permuted PPNE (YaeF/YiiX-like and LRAT-like) subsets (47). Both CPNE and PPNE families have similar tertiary structures, but in PPNEs, the residue order of the active site triad (His/Cys/polar) is swapped (41, 47). The cysteine/histidine dyad needed to form the covalent acyl-thioster substrate-enzyme intermediate in the NlpC/P60 superfamily active site is invariant (52, 53). CPNEs are common in prokaryotes, acting as extracellular hydrolases, peptidases, and amidases that remodel peptidoglycan (54, 55). The functions of the bacterial PPNEs (YaeF/YiiX-like) are poorly understood (47). Although the overall sequence similarity with LnsA is modest, all five HHPred homology hits are PPNEs, and the corresponding permuted active site residues in LnsA can be inferred (Fig. 6A). Interestingly, YiiX endogenously cocrystallized with a fatty acid in a hydrophobic S1 binding pocket that appears to be conserved in PPNEs (47). Unlike the prokaryotic YaeF/YiiX-like PPNE subfamily, the LRAT (lecithin:retinol acyl transferase-like enzymes) are a diverse group of enzymes in vertebrates with well-established functions in glycerophospholipid remodeling metabolism (48). Three of the top five proteins with similarity to LnsA are H-RAS-like suppressor (HRASLS) family members, a group of enzymes with shared phospholipase $A_{1/2}$ ($PLA_{1/2}$) hydrolase activity, as well as *O*- and *N*-acyltransferase activity (56, 57). HRASLS-2, HRASLS-3, and HRASLS-4 all have $PLA_{1/2}$ hydrolase activity *in vitro* and, in the case of HRASLS-2/HRASLS-3, also have *N*-acyltransferase activity that utilizes a phosphatidylcholine acyl chain donor to convert phosphatidylethanolamine into *N*-acyl phosphatidylethanolamine (57–59). The latter activity, in particular, has

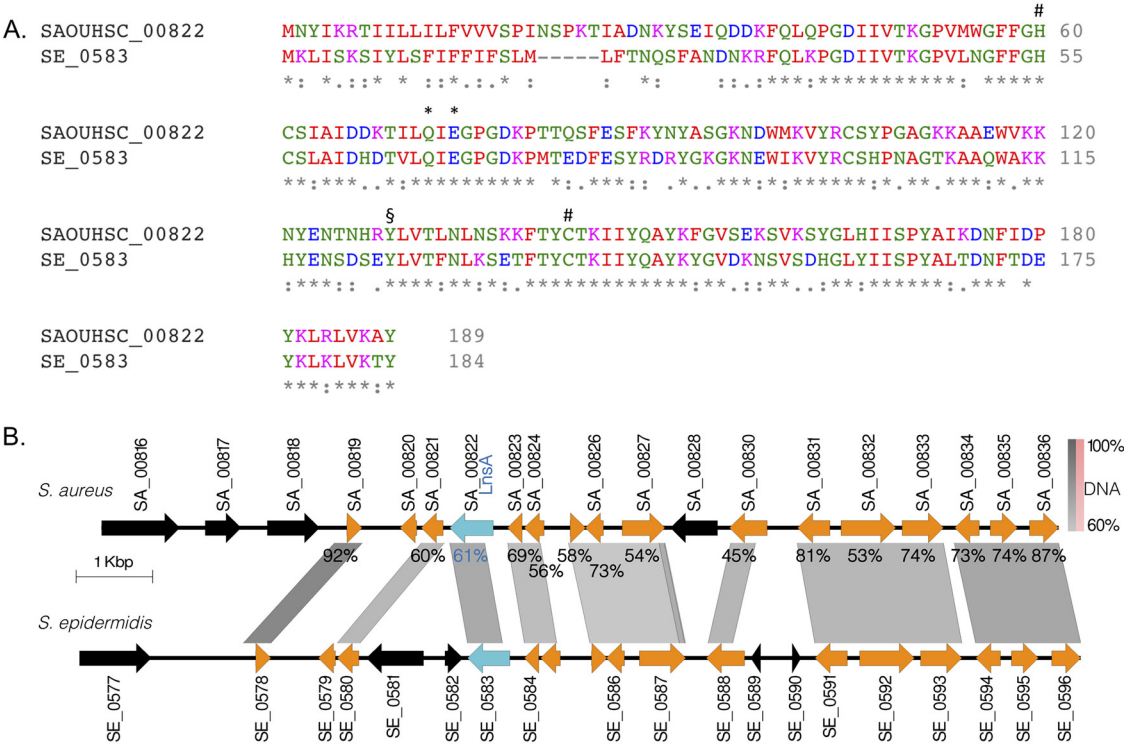

FIG 6 Bioinformatic analysis of LnsA orthologs in staphylococci. (A) An alignment of the characterized LnsA (SAOUHSC_00822) protein from *S. aureus* with the SE_0583 ortholog from *S. epidermidis* ATCC 12228 was created using Clustal Ω (97). The *S. aureus* and *S. epidermidis* proteins share 61% amino acid identity. The genome of *S. carnosus* TM300 has no open reading frames with significant similarity. The four important catalytic residues in PPNEs equivalent to those in papain are indicated: invariant histidine/cysteine dyad residues (#), the NlpC/P60 protein superfamily tyrosine signature residue (§), and two candidates for the third active site polar residue (*) (47). (B) The genetic loci for each staphylococcus strain were aligned by DNA sequence homology centered around the respective LnsA open reading frame (LnsA from *S. aureus* and SE_0583 in *S. epidermidis* ATCC 12228) and are indicated in blue. Regions with DNA homology (% identical base pairs indicated by bar scale) are indicated in gray. Genes common to both species are indicated in orange, and genes without orthologs in the genomic region shown are black. The percent amino acid sequence identity is indicated for each similar locus tag gene pair. Plot was constructed using EasyFig (98).

strong parallels with the biochemistry required for Lpp *N*-acylation and makes LnsA the more obvious catalytic candidate for acyl transferase activity. Among the three *Staphylococcus* species with experimentally characterized Lpp structures (*S. aureus* TA-Lpp, *S. epidermidis* TA-Lpp, and *S. carnosus* *N*-acetyl-Lpp), LnsA orthologs are only present in the genomes of *S. aureus* and *S. epidermidis*, with a common genome synteny and sequence conservation at both the DNA and the protein level (61% identity, Fig. 6B).

Aside from being absolutely required for TA-Lpp formation (Fig. 3 and 4) and TLR2/1 specific detection in *S. aureus* (Fig. 1B, 2, and 5) or *L. monocytogenes* when heterogeneously expressed (Fig. 1C), the function of LnsB in Lpp *N*-acylation is much more speculative than LnsA. LnsB does have very weak similarity to the CAAX prenyl protease from the archaeal methanogen *Methanococcus maripaludis* (Rce1 [4CAD_C] [60], 14% identity) and the APH-1A subunit of human γ-secretase (APH-1A [5A63_C] [61], 7% identity). Both of these integral membrane proteins are part of the CAAX protease and bacteriocin-processing enzyme (CPBP) family (62), a large class of enzymes encompassing metalloproteases and other integral membrane proteins with poorly defined cellular function. Many bacteria encode multiple CPBPs, with *S. aureus* NCTC8325 containing at least six other CPBP enzymes in addition to LnsB (62). Of these, MroQ is a suspected protease that processes auto-inducing peptide (63, 64). There is phenotypic evidence for roles of four other staphylococcal CPBPs in maintaining cell envelope integrity (65) and in the expression of cell wall-attached surface proteins with YSIRK peptide signals (66). It is apparent from these studies, however, that the cellular functions are not entirely overlapping, and at least one (SAOUHSC_02611/LyrA/SpdC)

is almost certainly not a protease since key catalytic residues are absent (67). A similar analysis of catalytic motifs in LnsB shows considerable divergence from all CPBP-subfamily signature motifs as well, particularly in motif 4 (Fig. S5A). The similarity of LnsB to CAAX proteases, albeit without conservation of catalytic residues, suggests the CPBP fold could have been coopted for a noncatalytic chaperone role analogous to that suggested for the APH-1 subunit of γ-secretase (68). APH1 has low sequence conservation of CPBP catalytic residues like LnsB (Fig. 6A) and no standalone proteolytic activity. Instead, APH1 is proposed to present protein substrate to the presenilin protease subunit core for hydrolysis within the γ-secretase complex (69). Whether LnsB physically associates with LnsA in a complex, contributes any catalytic residues to the active site, or interacts with Lpp substrates remains to be determined. Alternative models where LnsB makes a novel acyl donor that is used by LnsA or where LnsB is indirectly required to process or stabilize LnsA cannot be ruled out.

There are also substantial differences in gene content and arrangement between the *S. aureus* LnsB genomic locus and the corresponding positions in both *S. epidermidis* and *S. carnosus* genomes. Genomic synteny in the LnsB loci between the staphylococci strains is highly mosaic, suggesting possible species-specific recombination or even horizontal acquisition events (Fig. S5B). While *S. aureus* (TA-Lpp) has common flanking genes with *S. epidermidis* (TA-Lpp) and *S. carnosus* (*N*-acetyl Lpp) on only one side, they are inverted with respect to LnsB (Fig. S5B). Gene architecture in *S. epidermidis* is intermediate and shares certain features with both genomes. Curiously, an LnsB-like CPBP open reading frame in the same position is present in all three genomes, including in the *N*-acetyl Lpp forming *S. carnosus* genome (SCA_1941). The overall sequence similarity between all three CPBP proteins is much lower (25 to 28% identical) though, in comparison to neighboring genome segments, which is inconsistent with expectations for simple species-driven genetic drift. Once more, no homology can be detected between the CPBP open reading frames at the DNA level, suggesting functional divergence as well as a possibly independent origin for all three genes. As with LnsB from *S. aureus*, the *S. epidermidis* ortholog (SE_2027) does not have many of the essential CPBP catalytic motifs and thus likely functions in Lpp *N*-acylation as well (Fig. S5A). The *S. carnosus* CPBP gene (SCA_1941) in comparison has all the CBPB canonical signature residues, including a completely intact motif 4. The sequence divergence may reflect the difference in catalytic activity (Lpp *N*-acetylation versus *N*-acylation) or, more likely, that SCA_1941 is not a functional LnsB ortholog and that the seemingly conserved synteny is due to genome rearrangement events.

The identification of LnsAB expands the catalog of known TLR2 recognition factors for staphylococci (Fig. 5). The TLR2-stimulating potential between different *Firmicutes*, and even within the same species, can vary significantly (11). In *S. aureus*, differences in total Lpp gene content, capsular polysaccharide thickness, and autolysis rates can all attenuate ligand release and accessibility (70). Phenol soluble modulins produced by *S. aureus* are surfactant-like small peptides that enhance release of Lpp-loaded extracellular vesicle release and in turn alter TLR2 responses (71). Disparity also stems from TLR2 antagonizing factors. The lipoylated E2 subunit of the pyruvate dehydrogenase complex suppresses TLR2/1 activity (72), while levels of secreted lipases that degrade shed Lpp is subject to lysogenic bacteriophages (73). An additional factor is the Lpp chemotype itself, which can indirectly attenuate the TLR2 response by acting through any of the above mechanisms, or more simply by altering ligand specificity and/or affinity at the respective TLR2 receptor complexes as demonstrated here. It should be noted that in staphylococci there are no other compounds described that activate TLR2 and Lpp is the dominant immunobiologically active ligand (23, 74).

Although TLR2 attenuation is clearly an outcome of chemotype conversion from DA-Lpp to TA-Lpp, there is likely an overarching selective pressure for Lpp *N*-modification that supersedes immune evasion. Noncommensal strains such as *S. carnosus* and environmental strains such as *B. subtilis* have Lpps modified with *N*-acetyl groups. Analogous *N*-acetyl amino terminal tailoring has even been reported in archaea (75). Some archaea express Lpp-like, membrane-associated proteins with a characteristic

lipobox preceding an invariant cysteine residue as in bacteria, except that they are thought to be modified with diphytanoyl glycerol diether lipid (76). TLR2 immunomodulation is an unlikely motivation for N-terminal tailoring in any of these cases. One possible clue regarding a broader, universal selective pressure operating outside the host TLR2-bacterial niche is offered by the recent discovery of an Lit2 paralog in *L. monocytogenes* (21). The *lit2* gene is embedded within a copper resistance operon on either a transposon or transmissible plasmid in select environmental isolates. Like chromosomally encoded Lit, Lit2 converts DA-Lpp to lyso-Lpp but is specifically induced by copper ions. It was suggested that Lpp *N*-acylation may help prevent copper coordination at the membrane surface, limiting its uptake or oxidative damage from copper-mediated redox cycling (21). In *E. coli*, copper exposure induces DA-Lpp accumulation and Lpp outer membrane trafficking defects (77), while intracellular copper accumulates in Lnt depletion strains (78). Copper as a selective pressure would help explain the genesis of novel Lpp acylation systems such as LnsAB and more broadly the Lpp chemotype heterogeneity observed in *Firmicutes*. Copper selective pressure has grown in step with environmental oxygenation levels that increase copper bioavailability (79). Contemporary selection for copper resistance determinants has also arisen from copper's widespread current use as an antimicrobial agent (80). Assuming that the core Lgt-Lsp pathway was initially established in prokaryotes and that selective pressure for Lpp *N*-acylation arose after establishment of the various lineages, different bacterial species would have subsequently acquired *N*-acylation systems independently from each other. A particularly intriguing theory proposes modern *Firmicute* monoderm lineages independently arose at multiple times from a common diderm ancestor through loss of genes directing the biogenesis of the second outer membrane (81, 82). If a common ancestral Lpp *N*-acylation system was lost in tandem, multiple independent Lpp *N*-acylating gene reacquisition events would have followed. In either case, the Lpp *N*-acylation system diversity exemplified by LnsAB has provided a ready-made genetic reservoir to modulate TLR2-mediated immunodetection among *Firmicutes*.

MATERIALS AND METHODS

Bacterial strains and growth conditions. All *E. coli* strains were grown in lysogeny broth-Miller medium (LB), while *S. aureus* and *L. monocytogenes* strains were grown in tryptic soy broth (TSB) at 37°C in baffled flasks (3-to-1 flask to culture ratio) with continuous aeration at 250 rpm unless indicated otherwise. For cytokine production assays, *S. aureus* strains were cultivated in basic medium (BM; 1% soy peptone, 0.5% yeast extract, 0.5% NaCl, 0.1% glucose, and 0.1% K_2HPO_4 [pH 7.2]) at 37°C under continuous shaking at 150 rpm. Antibiotic resistance markers were selected with carbenicillin (100 μg/ml), kanamycin (30 μg/ml), spectinomycin (50 μg/ml), chloramphenicol (20 μg/ml in *E. coli*, 10 μg/ml for plasmid or 5 μg/ml for integrated marker in *S. aureus*, and 3 μg/ml in *L. monocytogenes*), and erythromycin (5 μg/ml) where appropriate. The *S. aureus* NCTC8325 HG003 transposon library, built in the derivative strain TM226 (30), and the Nebraska Transposon Mutant Library (NTML), built in *S. aureus* strain USA300 (83), were cultured in 96-well microplates with buffered TSB (50 mM HEPES [pH 7.4]) without shaking in a humidified environment at 37°C. For pET22-based vectors, gene expression was induced using 1 mM IPTG (isopropyl-β-D-thiogalactopyranoside). For expression of xylose-inducible genes encoded in plasmid pCX30, BM medium was supplemented with 10 μg/ml chloramphenicol, and glucose was substituted by 0.5% (wt/vol) xylose. Generation times were measured in 96-well microplates in TSB media incubated at 37°C. All strains and plasmids are listed in Table 1.

Construction of bacterial deletion strains and plasmids. Gene deletions were constructed using the temperature-sensitive shuttle vector pKFC in *S. aureus*, as previously described (84, 85). Plasmids were assembled from two separate 1-kb DNA fragments flanking the gene targeted for deletion and obtained by PCR. About 10 coding triplets from both ends of the targeted gene were retained to create nonpolar, in-frame gene deletions. Fragments were assembled using the In-Fusion HD cloning kit (TaKaRa Bio) and transformed into restriction negative *S. aureus* RN4220 by electroporation. Plasmids were then isolated and also transformed into strains TM226 and JE2 for integration and outcross in these genetic backgrounds. Deletion alleles were confirmed by PCR using primers annealing outside the targeted locus (Fig. S6). Complementation plasmids expressing SAOUHSC_00822, SAOUHSC_02761, or both genes in tandem were built from fragments amplified from *S. aureus* NCTC8325 genomic DNA and cloned into pLI50 (86), pCN59 (87), or pET22 (Novagen) using the same method and verified by sequencing. Expression of *S. aureus* genes in *L. monocytogenes* was achieved by integration into the chromosome using the pPL2 integration vector (88). The xylose-inducible pCX30 based complementation vectors (89) were constructed by PCR amplifying the two genes (SAUSA300_0780 and SAUSA300_2405) from *S. aureus* USA300 genomic DNA. The PCR inserts were cloned into pCX30 linearized with BamHI and SmaI using Hi-Fi DNA Assembly Master Mix (New England Biolabs). The resulting plasmid was transformed into *S. carnosus* TM300 by electroporation. Plasmid-harboring colonies were picked and verified by DNA

TABLE 1 Bacterial strains and plasmids used in this study

Strain or plasmid	Relevant genotype and/or phenotype[a]	Source or reference
Strains		
E. coli		
BW25113	*E. coli* K-12 wild type; Δ(*araD araB*)*567* Δ*lacZ4787*(::*rrnB-3*) λ⁻ *rph-1* Δ(*rhaD-rhaB*)*568 hsdR514*	CGSC7636[b]
KA327	BW25113 Δ*lpp*	20
KA548	*lpp*::Cm^r + pCL25 ori-pKD4 kanR-lppK58A-strep; synthesizes triacylated Lpp that cannot be covalently cross-linked to peptidoglycan	20
KA775	*lpp*::Cm^r *lnt*::Spec^r + pKA522-PA3286 (pCL25 ori-kanR-lppK58A strep-PA3286) (spontaneous suppressor mutant); synthesizes diacylated Lpp that cannot be covalently cross-linked to peptidoglycan	46
S. aureus		
TM226	*S. aureus* HG003 NCTC8325 ϕ11::FRT	30
Tn 16C2	TM226 Tn insertion 18-bp upstream of SAOUHSC_02761 start codon, Erm^r	This study
Tn 32F1	TM226 Tn insertion in amino acid 114 of SAOUHSC_02761, Erm^r	This study
JG1299	TM226 *lsp*::Tn, Erm^r	This study
JG1300	TM226 *lgt*::Tn, Erm^r	This study
JG1497	TM226 ΔSAOUHSC_02761	This study
JG1498	TM226 ΔSAOUHSC_00822	This study
JG1499	TM226 ΔSAOUHSC_00822 ΔSAOUHSC_02761	This study
TXM1515	JG1497 + pCN59 P_{nat} SAOUHSC_02761, Erm^r	This study
TXM1516	JG1498 + pCN59 P_{nat} SAOUHSC_00822, Erm^r	This study
TXM1523	JG1499 + p*Bc* Lit, Cm^r; synthesizes lyso-form Lpps, Cm^r	This study
TXM1529	JG1499 + pCN59 P_{nat} SAOUHSC_02761 SAOUHSC_00822, Erm^r	This study
RN4220	*S. aureus* NCTC8325 restriction negative, prophage cured	94
TXM1485	RN4220 ΔSAOUHSC_02761	This study
TXM1486	RN4220 ΔSAOUHSC_00822	This study
TXM1500	RN4220 ΔSAOUHSC_02761 ΔSAOUHSC_00822	This study
TXM1510	TXM1486 + pCN59 P_{nat} SAOUHSC_00822, Erm^r	This study
TXM1511	TXM1485 + pCN59 P_{nat} SAOUHSC_02761, Erm^r	This study
TXM1528	TXM1500 + pCN59 P_{nat} SAOUHSC_02761 SAOUHSC_00822, Erm^r	This study
TXM1577	TXM1500 + pLI50-sitC10AA, Cm^r	This study
TXM1578	TXM1486 + pLI50-sitC10AA, Cm^r	This study
TXM1579	RN4220 + pLI50-sitC10AA, Cm^r	This study
TXM1580	TXM1577 + pCN59 P_{nat} SAOUHSC_02761 SAOUHSC_00822, Cm^r Erm^r	This study
TXM1581	TXM1578 + pCN59 P_{nat} SAOUHSC_00822, Cm^r Erm^r	This study
TXM1582	TXM1583 + pCN59 P_{nat} SAOUHSC_02761, Cm^r Erm^r	This study
TXM1583	TXM1485 + pLI50-sitC10AA, Cm^r	This study
TXM1584	TXM1577 + pCN59 P_{nat} SAOUHSC_00822, Cm^r Erm^r	This study
TXM1585	TXM1577 + pCN59 P_{nat} SAOUHSC_02761, Cm^r Erm^r	This study
TXM1586	TXM1577 + pCN59 P_{pen} SAOUHSC_00822, Cm^r Erm^r	This study
TXM1587	TXM1577 + pCN59 P_{pen} SAOUHSC_02761, Cm^r Erm^r	This study
TXM1588	TXM1577 + pCN59 P_{pen} SAOUHSC_02761 SAOUHSC_00822, Cm^r Erm^r	This study
JE2	*S. aureus* USA300 wild-type cure of endogenous plasmids	BEI
NE536	SAUSA300_0780::Tn, Erm^r	BEI
NE407	SAUSA300_2405::Tn, Erm^r	BEI
L. monocytogenes		
Wild type	*L. monocytogenes* Li2 ATCC 19115	ATCC[c]
TXM1530	*att*::pPL2-P_{pen} SAOUHSC_00822	This study
TXM1531	*att*::pPL2-P_{pen} SAOUHSC_02761	This study
TXM1532	*att*::pPL2-P_{pen} SAOUHSC_02761 and SAOUHSC_00822	This study
S. carnosus		
Wild type	*S. carnosus* strain TM300	95
Plasmids[d]		
pLI50	*E. coli-S. aureus* shuttle vector, Carb^r Cm^r	86
pLI50-PpenGfpmut2	pLI50 with P_{pen} insert to control expression; Carb^r Cm^r	96
pLI50-sitC10AA	pLI50-P_{tuf} SitC N terminus 10-amino-acid fragment-strep tag TT	This study
pCN59	*E. coli-S. aureus* shuttle vector, Carb^r Erm^r	87
pGKM1456	pCN59 P_{nat} SAOUHSC_00822, Carb^r Erm^r	This study
pTXM1505	pCN59 P_{nat} SAOUHSC_02761, Carb^r Erm^r	This study
pTXM1508	pCN59 P_{pen} SAOUHSC_00822, Carb^r Erm^r	This study
pTXM1509	pCN59 P_{pen} SAOUHSC_02761, Carb^r Erm^r	This study
pTXM1512	pCN59 P_{pen} SAOUHSC_02761 SAOUHSC_00822, Carb^r Erm^r	This study
p*Bc*Lit	pLI50 P_{pen} *Bacillus cereus lit* gene, Carb^r Cm^r	This study
pTXM1524	pCN59 P_{nat} SAOUHSC_02761 SAOUHSC_00822, Carb^r Erm^r	This study
pPL2	*E. coli* shuttle-*L. monocytogenes* integration vector, Cm^r	88

(Continued on next page)

TABLE 1 (Continued)

Strain or plasmid	Relevant genotype and/or phenotype[a]	Source or reference
pTXM1525	pPL2-P_{pen} SAOUHSC_00822, Cm^r	This study
pTXM1526	pPL2-P_{pen} SAOUHSC_02761, Cm^r	This study
pTXM1527	pPL2-P_{pen} SAOUHSC_02761 SAOUHSC_00822, Cm^r	This study
pTXM908	pBBR1 ori P_{Kan}-*lolCDE*	46
pCX30	pC194 ori, P_{xyl} to control expression, Cm^r	89
pCX-LnsA/LnsB	pCX30 P_{xyl} LnsA (SAUSA300_0780) and LnsB (SAUSA300_2405), Cm^r	This study
pCX-LnsA	pCX30 P_{xyl} LnsA (SAUSA300_0780), Cm^r	This study
pCX-LnsB	pCX30 P_{xyl} LnsB (SAUSA300_2405), Cm^r	This study

[a]Resistance phenotypes: Carb^r, carbenicillin; Cm^r, chloramphenicol; Kan^r, kanamycin; Erm^r, erythromycin resistance; Spec^r, spectinomycin.
[b]Strain CGSC7636 at the Coli Genetic Stock Center (CGSC).
[c]American Type Culture Collection.
[d]TT, transcriptional terminator.

sequencing. The correct plasmid was then transformed into wild type [JE2 (pCX-LnsA/LnsB)]. The Tn mutant strains from the NTML library [NE536(pCX-LnsA) and NE407(pCX-LnsB)] were complemented using single-gene-expressing vectors constructed in the same way. All primers are listed in Table S1 in the supplemental material.

Transposon library screening for TLR2 activity. Screens for Tn mutants modulating TLR2 signaling were conducted with two libraries: (i) our in-house Tn library constructed and described by Santiago et al. using *S. aureus* NCTC8325 strain TM226 (30) and (ii) the NTML built in *S. aureus* strain USA300 JE2 (83). For the TM226 transposon library, the glycerol stock Tn pool was diluted and streaked to single colonies on tryptic soy agar (TSA; 5 μg/ml erythromycin) and incubated overnight at 37°C. The next morning, individual colonies were inoculated into buffered TSB (200 μl/well with 5 μg/ml erythromycin) distributed in 96-well plates. Controls were included on each microplate (*S. aureus* RN4220 wild type and medium only). Microplates were incubated for 18 h at 37°C without agitation before bacterial cultures were resuspended by pipetting up and down three times. Aliquots (20 to 50 μl) were transferred to a 96-well PCR plate, and bacteria were heat killed by incubation at 58°C for 1 h. The NTML screen was conducted in an identical manner, except that the growth microplates were inoculated with 5 μl of thawed glycerol stocks from the prearrayed library stock plate. Heat-killed bacterial extracts were stored at 4°C until use.

Human embryonic kidney 293 cells (HEK-Blue hTLR2-TLR1; Invivogen) with endogenous TLR1 and TLR6 deleted and stably transfected with TLR2, TLR1, and an NF-κB responsive secreted alkaline phosphatase reporter gene were cultured as recommended by the manufacturer and recently described (90). On the day of the assay, ~70% confluent HEK-Blue hTLR2-TLR1 cells were washed with 1× phosphate-buffered saline (PBS), harvested by centrifugation, counted, and diluted to the recommended final concentration of ~280,000 cells/ml in Dulbecco modified Eagle medium (DMEM) without selective antibiotics. To each well containing 190 μl of cell culture medium, 10 μl of the heat-killed bacterial extract was added. Microplates were then incubated at 37°C in a 5% CO_2 atmosphere for 44 h (for TLR2/1 assays), which pilot studies determined to be optimal for the largest dynamic assay range. Secreted alkaline phosphate was assayed as described previously (90), with minor modifications. Aliquots (20 μl) of supernatant were removed and added to 180 μl of QuantiBlue detection reagent (Invivogen), followed by incubation for 4 h before the absorbance was measured at 620 nm. Defined TLR2 Lpp ligands prepared from *E. coli* cells expressing either TA-Lpp (KA548) or DA-Lpp (KA775) were used as stimulation controls.

Primary Tn mutant hits were struck to single colonies and the decrease in TLR2/1 activity assay results confirmed. These samples were then tested for retention of TLR2/6 specific activity using HEK-Blue hTLR2-TLR6 cells (Invivogen) as described above except cells were stimulated for 20 h. All genotypes were checked and confirmed by PCR using primers targeting the *lgt*, *lsp*, and candidate *N*-acylation genes in the prearrayed NTML (Fig. S7). For the TM226 library (Fig. S1E), Tn insertion sites were mapped by inverse PCR of circularized gDNA fragments, as described elsewhere, except that *Taq*αI (New England Biolabs) was used for DNA restriction (91).

TLR2 dose-response HEK-Blue reporter assays. The TLR2 stimulating activity of Lpp *N*-acylation mutants was assayed using HEK-Blue hTLR2 (TA-Lpp and DA-Lpp responsive), HEK-Blue hTLR2-TLR1 (TA-Lpp responsive), and HEK-Blue hTLR2-TLR6 (DA-Lpp responsive) cells cultured and assayed as described above. Serial dilutions of heat-killed bacterial extracts were prepared as described above except bacterial cultures were grown to mid-log-growth phase (optical density at 600 nm [OD_{600}] of 1.0 to 1.5) with aeration in 14-ml culture tubes to limit accumulation of DA-Lpp during stationary phase (92). CFU/ml were obtained by plating three different dilutions of cultures on TSA and enumerating colonies after overnight incubation.

Total RNA Northern blotting. Northern blots were performed using a NorthernMax kit (Ambion) according to the manufacturer's instructions. Briefly, 1.5 μg of total RNA for each strain of *S. aureus* were separated on a 1% MOPS (morpholinepropanesulfonic acid)-formaldehyde-agarose gel and transferred to a BrightStar-Plus positively charged nylon membrane (Invitrogen) using a Whatman Nytran SuPerCharge TurboBlotter kit (GE Healthcare Life Sciences) for 3.5 h. Samples were cross-linked to the membrane by baking at 80°C for 20 min. Biotin-labeled RNA probes were synthesized

from DNA with gene-T7-specific primer sets (see Table S1 in the supplemental material) using a MaxiScript T7 transcription kit (Thermo Fisher), including the optional DNase digestion and cleanup with NucAway spin columns (Invitrogen). Probes were added to 10 ng/ml in Ultrahyb ultrasensitive hybridization buffer (Invitrogen), followed by incubation at 72°C for 16 h. The membranes were washed as directed using a NorthernMax kit, with the two high-stringency washes performed at 68°C. RNA was visualized with a chemiluminescent nucleic acid detection kit (Thermo Fisher) according to the manufacturer's instructions.

Immunoblotting for strep-tagged Lpp probe. A plasmid expressing a 10-amino-acid fragment of the SitC Lpp with a C-terminal strep epitope under the control of the strong constitutive promoter P_{tuf} was constructed in the shuttle vector pLI50. The plasmid pLI50-sitC10AA was transformed into various RN4220 strains, and cultures were grown to early log phase (OD_{600} = 0.5). Bacterial pellets were obtained by centrifugation, washed once with PBS, and resuspended in buffer (10 mM Tris-HCl [pH 8.0]) containing 50 μg/ml of lysostaphin. Samples were incubated for 15 min at 37°C before being quenched with 4× SDS-PAGE loading buffer. Samples were then heated at 70°C for 15 min before being clarified by centrifugation (18,000 × *g*, 5 min). Aliquots of supernatant were loaded onto an 18% Tris-tricine minigel and separated by electrophoresis using the Tris-tricine running buffer system (93). Protein was transferred to a nitrocellulose membrane (0.2 μM) and developed with an HRP-anti-strep tag conjugate as instructed by the manufacturer (StrepMAB-Classic HRP conjugate; IBA Life Sciences).

MALDI-TOF mass spectrometry. Lpps were prepared for mass spectrometry as previously described (20, 43). Briefly, Lpps were extracted using the Triton X-114 phase partitioning method, separated with a 10% SDS-PAGE gel, and transferred to a nitrocellulose membrane. Bands corresponding to *S. aureus* SitC (SAOUHSC_00634) and to a periplasmic binding protein type 2 family (SAOUHSC_02699) lpp were trypsinized overnight. After elution from the membranes, samples were mixed with α-cyano-4-hydroxycinnamic acid (α-CHCA) matrix and analyzed on an Ultraflextreme (Bruker Daltonics) MALDI-TOF mass spectrometer in positive reflector mode. MS-MS spectra were acquired in Lift mode.

Cytokine release assay. The cultivation of HEK-Blue hTLR2 cells and bacterial preparation for the stimulation assay were performed as described previously (23). Cells were cultured in DMEM (Thermo Fisher) supplemented with 10% fetal bovine serum, 50 mg/liter Normocin (InvivoGen), and 1× HEK-Blue Selection (InvivoGen) at 37°C with 5% CO_2 supplementation. HEK-Blue hTLR2 cells were seeded with 5×10^4 cells/200 μl/well into 96-well cell culture plates, followed by incubation at 37°C with 5% CO_2 for 24 h. Bacterial cells from overnight culture with antibiotics added according to plasmids being carried (Fig. S8) were harvested and washed three times with Dulbecco PBS (DPBS) before measuring the OD_{578} in DPBS. To calculate bacterial dosage (MOI [multiplicity of infection]), bacteria were set to OD_{578} of 1.0, which equals 1×10^8 CFU/ml. The final bacterial dosage (MOI of 2) was suspended in 50 μl of the HEK-Blue hTLR2 medium and added to the cultured HEK-Blue hTLR2 cells (total volume of medium, 200 μl). Stimulation by these bacteria was carried out for 18 h before cellular supernatants were collected for cytokine assays. IL-8 secreted was measured by using an IL-8 human ELISA kit (Thermo Fisher) according to the manufacturer´s instruction.

SUPPLEMENTAL MATERIAL

Supplemental material is available online only.

TABLE S1, DOCX file, 0.03 MB.

FIG S1, TIF file, 0.6 MB.

FIG S2, TIF file, 1 MB.

FIG S3, TIF file, 2.7 MB.

FIG S4, TIF file, 2.8 MB.

FIG S5, TIF file, 1.8 MB.

FIG S6, TIF file, 0.5 MB.

FIG S7, TIF file, 0.3 MB.

FIG S8, TIF file, 0.3 MB.

ACKNOWLEDGMENTS

We thank Tatiana Laremore and Julia Fecko (Penn State Proteomics and Mass Spectrometry Core Facility, University Park, PA) for technical advice.

This study was funded by the National Institutes of Health (R01GM127482 to T.C.M.). F.G. and M.M. received infrastructural funding from the Deutsche Forschungsgemeinschaft and Cluster of Excellence EXC 2124 Controlling Microbes to Fight Infections. The following reagent was provided by the Network on Antimicrobial Resistance in *Staphylococcus aureus* for distribution through BEI Resources, NIAID, NIH: Nebraska Transposon Mutant Library Screening Array, NR-48501.

REFERENCES

1. Nakayama H, Kurokawa K, Lee BL. 2012. Lipoproteins in bacteria: structures and biosynthetic pathways. FEBS J 279:4247–4268. https://doi.org/10.1111/febs.12041.
2. Narita S, Tokuda H. 2010. Biogenesis and membrane targeting of lipoproteins. EcoSal Plus 4. https://doi.org/10.1128/ecosalplus.4.3.7.
3. Sutcliffe IC, Harrington DJ, Hutchings MI. 2012. A phylum level analysis reveals lipoprotein biosynthesis to be a fundamental property of bacteria. Protein Cell 3:163–170. https://doi.org/10.1007/s13238-012-2023-8.
4. Braun V, Hantke K. 2019. Lipoproteins: structure, function, biosynthesis. Subcell Biochem 92:39–77. https://doi.org/10.1007/978-3-030-18768-2_3.
5. Graf A, Lewis RJ, Fuchs S, Pagels M, Engelmann S, Riedel K, Pané-Farré J. 2018. The hidden lipoproteome of *Staphylococcus aureus*. Int J Med Microbiol 308:569–581. https://doi.org/10.1016/j.ijmm.2018.01.008.
6. Shahmirzadi SV, Nguyen MT, Götz F. 2016. Evaluation of *Staphylococcus aureus* lipoproteins: role in nutritional acquisition and pathogenicity. Front Microbiol 7:1404. https://doi.org/10.3389/fmicb.2016.01404.
7. Schmaler M, Jann NJ, Ferracin F, Landolt LZ, Biswas L, Götz F, Landmann R. 2009. Lipoproteins in *Staphylococcus aureus* mediate inflammation by TLR2 and iron-dependent growth *in vivo*. J Immunol 182:7110–7118. https://doi.org/10.4049/jimmunol.0804292.
8. Schmaler M, Jann NJ, Götz F, Landmann R. 2010. Staphylococcal lipoproteins and their role in bacterial survival in mice. Int J Med Microbiol 300:155–160. https://doi.org/10.1016/j.ijmm.2009.08.018.
9. Tsuru T, Kobayashi I. 2008. Multiple genome comparison within a bacterial species reveals a unit of evolution spanning two adjacent genes in a tandem paralog cluster. Mol Biol Evol 25:2457–2473. https://doi.org/10.1093/molbev/msn192.
10. Tribelli PM, Luqman A, Nguyen MT, Madlung J, Fan SH, Macek B, Sass P, Bitschar K, Schittek B, Kretschmer D, Götz F. 2020. *Staphylococcus aureus* Lpl protein triggers human host cell invasion via activation of Hsp90 receptor. Cell Microbiol 22:e13111. https://doi.org/10.1111/cmi.13111.
11. Nguyen MT, Götz F. 2016. Lipoproteins of Gram-positive bacteria: key players in the immune response and virulence. Microbiol Mol Biol Rev 80:891–903. https://doi.org/10.1128/MMBR.00028-16.
12. Oliveira-Nascimento L, Massari P, Wetzler LM. 2012. The role of TLR2 in infection and immunity. Front Immunol 3:79. https://doi.org/10.3389/fimmu.2012.00079.
13. Deguine J, Barton GM. 2014. MyD88: a central player in innate immune signaling. F1000Prime Rep 6:97. https://doi.org/10.12703/P6-97.
14. Narayanan KB, Park HH. 2015. Toll/interleukin-1 receptor (TIR) domain-mediated cellular signaling pathways. Apoptosis 20:196–209. https://doi.org/10.1007/s10495-014-1073-1.
15. O'Neill LA, Bowie AG. 2007. The family of five: TIR-domain-containing adaptors in Toll-like receptor signalling. Nat Rev Immunol 7:353–364. https://doi.org/10.1038/nri2079.
16. Fukuda A, Matsuyama S, Hara T, Nakayama J, Nagasawa H, Tokuda H. 2002. Aminoacylation of the N-terminal cysteine is essential for Lol-dependent release of lipoproteins from membranes but does not depend on lipoprotein sorting signals. J Biol Chem 277:43512–43518. https://doi.org/10.1074/jbc.M206816200.
17. Jin MS, Kim SE, Heo JY, Lee ME, Kim HM, Paik SG, Lee H, Lee JO. 2007. Crystal structure of the TLR1-TLR2 heterodimer induced by binding of a tri-acylated lipopeptide. Cell 130:1071–1082. https://doi.org/10.1016/j.cell.2007.09.008.
18. Kang JY, Nan X, Jin MS, Youn SJ, Ryu YH, Mah S, Han SH, Lee H, Paik SG, Lee JO. 2009. Recognition of lipopeptide patterns by Toll-like receptor 2-Toll-like receptor 6 heterodimer. Immunity 31:873–884. https://doi.org/10.1016/j.immuni.2009.09.018.
19. Kurokawa K, Ryu KH, Ichikawa R, Masuda A, Kim MS, Lee H, Chae JH, Shimizu T, Saitoh T, Kuwano K, Akira S, Dohmae N, Nakayama H, Lee BL. 2012. Novel bacterial lipoprotein structures conserved in low-GC content gram-positive bacteria are recognized by Toll-like receptor 2. J Biol Chem 287:13170–13181. https://doi.org/10.1074/jbc.M111.292235.
20. Armbruster KM, Meredith TC. 2017. Identification of the lyso-form *N*-acyl intramolecular transferase in low-GC *Firmicutes*. J Bacteriol 199:e00099-17. https://doi.org/10.1128/JB.00099-17.
21. Armbruster KM, Komazin G, Meredith TC. 2019. Copper-induced expression of a transmissible lipoprotein intramolecular transacylase alters lipoprotein acylation and the Toll-like receptor 2 response to *Listeria monocytogenes*. J Bacteriol 201:e00195-19. https://doi.org/10.1128/JB.00195-19.
22. Nguyen MT, Kraft B, Yu W, Demircioglu DD, Demicrioglu DD, Hertlein T, Burian M, Schmaler M, Boller K, Bekeredjian-Ding I, Ohlsen K, Schittek B, Götz F. 2015. The νSaα specific lipoprotein-like cluster (Lpl) of *S. aureus* USA300 contributes to immune stimulation and invasion in human cells. PLoS Pathog 11:e1004984. https://doi.org/10.1371/journal.ppat.1004984.
23. Nguyen MT, Uebele J, Kumari N, Nakayama H, Peter L, Ticha O, Woischnig AK, Schmaler M, Khanna N, Dohmae N, Lee BL, Bekeredjian-Ding I, Götz F. 2017. Lipid moieties on lipoproteins of commensal and non-commensal staphylococci induce differential immune responses. Nat Commun 8:2246. https://doi.org/10.1038/s41467-017-02234-4.
24. Gupta SD, Wu HC. 1991. Identification and subcellular localization of apolipoprotein *N*-acyltransferase in *Escherichia coli*. FEMS Microbiol Lett 62:37–41. https://doi.org/10.1016/0378-1097(91)90251-5.
25. Robichon C, Vidal-Ingigliardi D, Pugsley AP. 2005. Depletion of apolipoprotein *N*-acyltransferase causes mislocalization of outer membrane lipoproteins in *Escherichia coli*. J Biol Chem 280:974–983. https://doi.org/10.1074/jbc.M411059200.
26. Wiktor M, Weichert D, Howe N, Huang CY, Olieric V, Boland C, Bailey J, Vogeley L, Stansfeld PJ, Buddelmeijer N, Wang M, Caffrey M. 2017. Structural insights into the mechanism of the membrane integral *N*-acyltransferase step in bacterial lipoprotein synthesis. Nat Commun 8:15952. https://doi.org/10.1038/ncomms15952.
27. Navarre WW, Daefler S, Schneewind O. 1996. Cell wall sorting of lipoproteins in *Staphylococcus aureus*. J Bacteriol 178:441–446. https://doi.org/10.1128/jb.178.2.441-446.1996.
28. Asanuma M, Kurokawa K, Ichikawa R, Ryu KH, Chae JH, Dohmae N, Lee BL, Nakayama H. 2011. Structural evidence of alpha-aminoacylated lipoproteins of *Staphylococcus aureus*. FEBS J 278:716–728. https://doi.org/10.1111/j.1742-4658.2010.07990.x.
29. Kurokawa K, Lee H, Roh KB, Asanuma M, Kim YS, Nakayama H, Shiratsuchi A, Choi Y, Takeuchi O, Kang HJ, Dohmae N, Nakanishi Y, Akira S, Sekimizu K, Lee BL. 2009. The triacylated ATP binding cluster transporter substrate-binding lipoprotein of *Staphylococcus aureus* functions as a native ligand for Toll-like receptor 2. J Biol Chem 284:8406–8411. https://doi.org/10.1074/jbc.M809618200.
30. Santiago M, Matano LM, Moussa SH, Gilmore MS, Walker S, Meredith TC. 2015. A new platform for ultra-high-density *Staphylococcus aureus* transposon libraries. BMC Genomics 16:252. https://doi.org/10.1186/s12864-015-1361-3.
31. Krogh A, Larsson B, von Heijne G, Sonnhammer EL. 2001. Predicting transmembrane protein topology with a hidden Markov model: application to complete genomes. J Mol Biol 305:567–580. https://doi.org/10.1006/jmbi.2000.4315.
32. Boyartchuk VL, Ashby MN, Rine J. 1997. Modulation of Ras and a-factor function by carboxyl-terminal proteolysis. Science 275:1796–1800. https://doi.org/10.1126/science.275.5307.1796.
33. Soding J, Biegert A, Lupas AN. 2005. The HHpred interactive server for protein homology detection and structure prediction. Nucleic Acids Res 33:W244–W288. https://doi.org/10.1093/nar/gki408.
34. Qi HY, Sankaran K, Gan K, Wu HC. 1995. Structure-function relationship of bacterial prolipoprotein diacylglyceryl transferase: functionally significant conserved regions. J Bacteriol 177:6820–6824. https://doi.org/10.1128/jb.177.23.6820-6824.1995.
35. Sankaran K, Wu HC. 1994. Lipid modification of bacterial prolipoprotein. Transfer of diacylglyceryl moiety from phosphatidylglycerol. J Biol Chem 269:19701–19706.
36. Hussain M, Ichihara S, Mizushima S. 1982. Mechanism of signal peptide cleavage in the biosynthesis of the major lipoprotein of the *Escherichia coli* outer membrane. J Biol Chem 257:5177–5182.
37. Raines LJ, Moss CW, Farshtchi D, Pittman B. 1968. Fatty acids of *Listeria monocytogenes*. J Bacteriol 96:2175–2177. https://doi.org/10.1128/JB.96.6.2175-2177.1968.
38. Sen S, Sirobhushanam S, Johnson SR, Song Y, Tefft R, Gatto C, Wilkinson BJ. 2016. Growth-environment dependent modulation of *Staphylococcus aureus* branched-chain to straight-chain fatty acid ratio and incorporation of unsaturated fatty acids. PLoS One 11:e0165300. https://doi.org/10.1371/journal.pone.0165300.
39. Lu YJ, Zhang YM, Grimes KD, Qi J, Lee RE, Rock CO. 2006. Acyl-

phosphates initiate membrane phospholipid synthesis in Gram-positive pathogens. Mol Cell 23:765–772. https://doi.org/10.1016/j.molcel.2006.06.030.
40. Parsons JB, Broussard TC, Bose JL, Rosch JW, Jackson P, Subramanian C, Rock CO. 2014. Identification of a two-component fatty acid kinase responsible for host fatty acid incorporation by *Staphylococcus aureus*. Proc Natl Acad Sci U S A 111:10532–10537. https://doi.org/10.1073/pnas.1408797111.
41. Anantharaman V, Aravind L. 2003. Evolutionary history, structural features and biochemical diversity of the NlpC/P60 superfamily of enzymes. Genome Biol 4:R11. https://doi.org/10.1186/gb-2003-4-2-r11.
42. Almagro Armenteros JJ, Tsirigos KD, Sonderby CK, Petersen TN, Winther O, Brunak S, von Heijne G, Nielsen H. 2019. SignalP 5.0 improves signal peptide predictions using deep neural networks. Nat Biotechnol 37:420–423. https://doi.org/10.1038/s41587-019-0036-z.
43. Armbruster KM, Meredith TC. 2018. Enrichment of bacterial lipoproteins and preparation of N-terminal lipopeptides for structural determination by mass spectrometry. J Vis Exp 21:56842. https://doi.org/10.3791/56842.
44. Stoll H, Dengjel J, Nerz C, Götz F. 2005. *Staphylococcus aureus* deficient in lipidation of prelipoproteins is attenuated in growth and immune activation. Infect Immun 73:2411–2423. https://doi.org/10.1128/IAI.73.4.2411-2423.2005.
45. Jackowski S, Rock CO. 1986. Transfer of fatty acids from the 1-position of phosphatidylethanolamine to the major outer membrane lipoprotein of *Escherichia coli*. J Biol Chem 261:11328–11333.
46. Armbruster KM, Komazin G, Meredith TC. 2020. Bacterial lyso-form lipoproteins are synthesized via an intramolecular acyl chain migration. J Biol Chem doi:10.1074/jbc.RA120.014000.
47. Xu Q, Rawlings ND, Chiu HJ, Jaroszewski L, Klock HE, Knuth MW, Miller MD, Elsliger MA, Deacon AM, Godzik A, Lesley SA, Wilson IA. 2011. Structural analysis of papain-like NlpC/P60 superfamily enzymes with a circularly permuted topology reveals potential lipid binding sites. PLoS One 6:e22013. https://doi.org/10.1371/journal.pone.0022013.
48. Golczak M, Kiser PD, Sears AE, Lodowski DT, Blaner WS, Palczewski K. 2012. Structural basis for the acyltransferase activity of lecithin:retinol acyltransferase-like proteins. J Biol Chem 287:23790–23807. https://doi.org/10.1074/jbc.M112.361550.
49. Wang L, Yu W, Ren X, Lin J, Jin C, Xia B. 2012. ^{1}H, ^{13}C, and ^{15}N resonance assignments of the N-terminal domain of human TIG3. Biomol NMR Assign 6:201–203. https://doi.org/10.1007/s12104-012-9357-2.
50. Ren X, Lin J, Jin C, Xia B. 2010. Solution structure of the N-terminal catalytic domain of human H-REV107–a novel circular permutated NlpC/P60 domain. FEBS Lett 584:4222–4226. https://doi.org/10.1016/j.febslet.2010.09.015.
51. Zimmermann L, Stephens A, Nam SZ, Rau D, Kubler J, Lozajic M, Gabler F, Soding J, Lupas AN, Alva V. 2018. A completely reimplemented MPI bioinformatics toolkit with a New HHpred server at its core. J Mol Biol 430:2237–2243. https://doi.org/10.1016/j.jmb.2017.12.007.
52. Golczak M, Palczewski K. 2010. An acyl-covalent enzyme intermediate of lecithin:retinol acyltransferase. J Biol Chem 285:29217–29222. https://doi.org/10.1074/jbc.M110.152314.
53. Xu Q, Sudek S, McMullan D, Miller MD, Geierstanger B, Jones DH, Krishna SS, Spraggon G, Bursalay B, Abdubek P, Acosta C, Ambing E, Astakhova T, Axelrod HL, Carlton D, Caruthers J, Chiu H-J, Clayton T, Deller MC, Duan L, Elias Y, Elsliger M-A, Feuerhelm J, Grzechnik SK, Hale J, Han GW, Haugen J, Jaroszewski L, Jin KK, Klock HE, Knuth MW, Kozbial P, Kumar A, Marciano D, Morse AT, Nigoghossian E, Okach L, Oommachen S, Paulsen J, Reyes R, Rife CL, Trout CV, van den Bedem H, Weekes D, White A, Wolf G, Zubieta C, Hodgson KO, Wooley J, Deacon AM, Godzik A, Lesley SA, Wilson IA. 2009. Structural basis of murein peptide specificity of a γ-D-glutamyl-l-diamino acid endopeptidase. Structure 17:303–313. https://doi.org/10.1016/j.str.2008.12.008.
54. Duchene MC, Rolain T, Knoops A, Courtin P, Chapot-Chartier MP, Dufrene YF, Hallet BF, Hols P. 2019. Distinct and specific role of NlpC/P60 endopeptidases LytA and LytB in cell elongation and division of *Lactobacillus plantarum*. Front Microbiol 10:713. https://doi.org/10.3389/fmicb.2019.00713.
55. Xu Q, Mengin-Lecreulx D, Liu XW, Patin D, Farr CL, Grant JC, Chiu HJ, Jaroszewski L, Knuth MW, Godzik A, Lesley SA, Elsliger MA, Deacon AM, Wilson IA. 2015. Insights into substrate specificity of NlpC/P60 cell wall hydrolases containing bacterial SH3 domains. mBio 6:e02327-14. https://doi.org/10.1128/mBio.02327-14.
56. Mardian EB, Bradley RM, Duncan RE. 2015. The HRASLS (PLA/AT) subfamily of enzymes. J Biomed Sci 22:99. https://doi.org/10.1186/s12929-015-0210-7.
57. Shinohara N, Uyama T, Jin XH, Tsuboi K, Tonai T, Houchi H, Ueda N. 2011. Enzymological analysis of the tumor suppressor A-C1 reveals a novel group of phospholipid-metabolizing enzymes. J Lipid Res 52:1927–1935. https://doi.org/10.1194/jlr.M015081.
58. Uyama T, Ikematsu N, Inoue M, Shinohara N, Jin XH, Tsuboi K, Tonai T, Tokumura A, Ueda N. 2012. Generation of *N*-acylphosphatidylethanolamine by members of the phospholipase A/acyltransferase (PLA/AT) family. J Biol Chem 287:31905–31919. https://doi.org/10.1074/jbc.M112.368712.
59. Uyama T, Jin XH, Tsuboi K, Tonai T, Ueda N. 2009. Characterization of the human tumor suppressors TIG3 and HRASLS2 as phospholipid-metabolizing enzymes. Biochim Biophys Acta 1791:1114–1124. https://doi.org/10.1016/j.bbalip.2009.07.001.
60. Manolaridis I, Kulkarni K, Dodd RB, Ogasawara S, Zhang Z, Bineva G, Reilly NO, Hanrahan SJ, Thompson AJ, Cronin N, Iwata S, Barford D. 2013. Mechanism of farnesylated CAAX protein processing by the intramembrane protease Rce1. Nature 504:301–305. https://doi.org/10.1038/nature12754.
61. Bai XC, Yan C, Yang G, Lu P, Ma D, Sun L, Zhou R, Scheres SHW, Shi Y. 2015. An atomic structure of human gamma-secretase. Nature 525:212–217. https://doi.org/10.1038/nature14892.
62. Pei J, Mitchell DA, Dixon JE, Grishin NV. 2011. Expansion of type II CAAX proteases reveals evolutionary origin of gamma-secretase subunit APH-1. J Mol Biol 410:18–26. https://doi.org/10.1016/j.jmb.2011.04.066.
63. Cosgriff CJ, White CR, Teoh WP, Grayczyk JP, Alonzo F, III. 2019. Control of *Staphylococcus aureus* quorum sensing by a membrane-embedded peptidase. Infect Immun 87:00019-19. https://doi.org/10.1128/IAI.00019-19.
64. Marroquin S, Gimza B, Tomlinson B, Stein M, Frey A, Keogh RA, Zapf R, Todd DA, Cech NB, Carroll RK, Shaw LN. 2019. MroQ is a novel Abi-domain protein that influences virulence gene expression in *Staphylococcus aureus* via modulation of Agr activity. Infect Immun 87:00002-19. https://doi.org/10.1128/IAI.00002-19.
65. Santa Maria JP, Jr, Sadaka A, Moussa SH, Brown S, Zhang YJ, Rubin EJ, Gilmore MS, Walker S. 2014. Compound-gene interaction mapping reveals distinct roles for *Staphylococcus aureus* teichoic acids. Proc Natl Acad Sci U S A 111:12510–12515. https://doi.org/10.1073/pnas.1404099111.
66. Frankel MB, Wojcik BM, DeDent AC, Missiakas DM, Schneewind O. 2010. ABI domain-containing proteins contribute to surface protein display and cell division in *Staphylococcus aureus*. Mol Microbiol 78:238–252. https://doi.org/10.1111/j.1365-2958.2010.07334.x.
67. Grundling A, Missiakas DM, Schneewind O. 2006. *Staphylococcus aureus* mutants with increased lysostaphin resistance. J Bacteriol 188:6286–6297. https://doi.org/10.1128/JB.00457-06.
68. Zhang X, Li Y, Xu H, Zhang YW. 2014. The gamma-secretase complex: from structure to function. Front Cell Neurosci 8:427. https://doi.org/10.3389/fncel.2014.00427.
69. Chen AC, Guo LY, Ostaszewski BL, Selkoe DJ, LaVoie MJ. 2010. Aph-1 associates directly with full-length and C-terminal fragments of gamma-secretase substrates. J Biol Chem 285:11378–11391. https://doi.org/10.1074/jbc.M109.088815.
70. Hilmi D, Parcina M, Stollewerk D, Ostrop J, Josten M, Meilaender A, Zaehringer U, Wichelhaus TA, Bierbaum G, Heeg K, Wolz C, Bekeredjian-Ding I. 2014. Heterogeneity of host TLR2 stimulation by *Staphylococcus aureus* isolates. PLoS One 9:e96416. https://doi.org/10.1371/journal.pone.0096416.
71. Schlatterer K, Beck C, Hanzelmann D, Lebtig M, Fehrenbacher B, Schaller M, Ebner P, Nega M, Otto M, Kretschmer D, Peschel A. 2018. The mechanism behind bacterial lipoprotein release: phenol-soluble modulins mediate Toll-like receptor 2 activation via extracellular vesicle release from *Staphylococcus aureus*. mBio 9:e01851-18. https://doi.org/10.1128/mBio.01851-18.
72. Grayczyk JP, Harvey CJ, Laczkovich I, Alonzo F, III. 2017. A lipoylated metabolic protein released by *Staphylococcus aureus* suppresses macrophage activation. Cell Host Microbe 22:678–687 e9. https://doi.org/10.1016/j.chom.2017.09.004.
73. Chen X, Alonzo F, III. 2019. Bacterial lipolysis of immune-activating ligands promotes evasion of innate defenses. Proc Natl Acad Sci U S A 116:3764–3773. https://doi.org/10.1073/pnas.1817248116.
74. Hashimoto M, Tawaratsumida K, Kariya H, Kiyohara A, Suda Y, Krikae F, Kirikae T, Götz F. 2006. Not lipoteichoic acid but lipoproteins appear to

be the dominant immunobiologically active compounds in *Staphylococcus aureus*. J Immunol 177:3162–3169. https://doi.org/10.4049/jimmunol.177.5.3162.
75. Mattar S, Scharf B, Kent SB, Rodewald K, Oesterhelt D, Engelhard M. 1994. The primary structure of halocyanin, an archaeal blue copper protein, predicts a lipid anchor for membrane fixation. J Biol Chem 269:14939–14945.
76. Eichler J, Maupin-Furlow J, Soppa J. 2010. Archaeal protein biogenesis: posttranslational modification and degradation. Archaea 2010:1–2. https://doi.org/10.1155/2010/643046.
77. May KL, Lehman KM, Mitchell AM, Grabowicz M. 2019. A stress response monitoring lipoprotein trafficking to the outer membrane. mBio 10: e00618-19. https://doi.org/10.1128/mBio.00618-19.
78. Rogers SD, Bhave MR, Mercer JF, Camakaris J, Lee BT. 1991. Cloning and characterization of *cutE*, a gene involved in copper transport in *Escherichia coli*. J Bacteriol 173:6742–6748. https://doi.org/10.1128/jb.173.21.6742-6748.1991.
79. Chi Fru E, Rodriguez NP, Partin CA, Lalonde SV, Andersson P, Weiss DJ, El Albani A, Rodushkin I, Konhauser KO. 2016. Cu isotopes in marine black shales record the Great Oxidation Event. Proc Natl Acad Sci U S A 113:4941–4946. https://doi.org/10.1073/pnas.1523544113.
80. Dalecki AG, Crawford CL, Wolschendorf F. 2017. Copper and antibiotics: discovery, modes of action, and opportunities for medicinal applications. Adv Microb Physiol 70:193–260. https://doi.org/10.1016/bs.ampbs.2017.01.007.
81. Antunes LC, Poppleton D, Klingl A, Criscuolo A, Dupuy B, Brochier-Armanet C, Beloin C, Gribaldo S. 2016. Phylogenomic analysis supports the ancestral presence of LPS-outer membranes in the *Firmicutes*. Elife 5:14589. https://doi.org/10.7554/eLife.14589.
82. Megrian D, Taib N, Witwinowski J, Beloin C, Gribaldo S. 2020. One or two membranes? Diderm *Firmicutes* challenge the Gram-positive/Gram-negative divide. Mol Microbiol 113:659–671. https://doi.org/10.1111/mmi.14469.
83. Yajjala VK, Widhelm TJ, Endres JL, Fey PD, Bayles KW. 2016. Generation of a transposon mutant library in *Staphylococcus aureus* and *Staphylococcus epidermidis* using bursa aurealis. Methods Mol Biol 1373:103–110. https://doi.org/10.1007/7651_2014_189.
84. Coe KA, Lee W, Stone MC, Komazin-Meredith G, Meredith TC, Grad YH, Walker S. 2019. Multi-strain Tn-Seq reveals common daptomycin resistance determinants in *Staphylococcus aureus*. PLoS Pathog 15:e1007862. https://doi.org/10.1371/journal.ppat.1007862.
85. Kato F, Sugai M. 2011. A simple method of markerless gene deletion in *Staphylococcus aureus*. J Microbiol Methods 87:76–81. https://doi.org/10.1016/j.mimet.2011.07.010.
86. Lee CY, Buranen SL, Ye ZH. 1991. Construction of single-copy integration vectors for *Staphylococcus aureus*. Gene 103:101–105. https://doi.org/10.1016/0378-1119(91)90399-v.
87. Charpentier E, Anton AI, Barry P, Alfonso B, Fang Y, Novick RP. 2004. Novel cassette-based shuttle vector system for gram-positive bacteria. Appl Environ Microbiol 70:6076–6085. https://doi.org/10.1128/AEM.70.10.6076-6085.2004.
88. Lauer P, Chow MY, Loessner MJ, Portnoy DA, Calendar R. 2002. Construction, characterization, and use of two *Listeria monocytogenes* site-specific phage integration vectors. J Bacteriol 184:4177–4186. https://doi.org/10.1128/jb.184.15.4177-4186.2002.
89. Yu W, Götz F. 2012. Cell wall antibiotics provoke accumulation of anchored mCherry in the cross wall of *Staphylococcus aureus*. PLoS One 7:e30076. https://doi.org/10.1371/journal.pone.0030076.
90. Komazin G, Maybin M, Woodard RW, Scior T, Schwudke D, Schombel U, Gisch N, Mamat U, Meredith TC. 2019. Substrate structure-activity relationship reveals a limited lipopolysaccharide chemotype range for intestinal alkaline phosphatase. J Biol Chem 294:19405–19423. https://doi.org/10.1074/jbc.RA119.010836.
91. Wang H, Claveau D, Vaillancourt JP, Roemer T, Meredith TC. 2011. High-frequency transposition for determining antibacterial mode of action. Nat Chem Biol 7:720–729. https://doi.org/10.1038/nchembio.643.
92. Kurokawa K, Kim MS, Ichikawa R, Ryu KH, Dohmae N, Nakayama H, Lee BL. 2012. Environment-mediated accumulation of diacyl lipoproteins over their triacyl counterparts in *Staphylococcus aureus*. J Bacteriol 194: 3299–3306. https://doi.org/10.1128/JB.00314-12.
93. Schagger H. 2006. Tricine-SDS-PAGE. Nat Protoc 1:16–22. https://doi.org/10.1038/nprot.2006.4.
94. Kreiswirth BN, Lofdahl S, Betley MJ, O'Reilly M, Schlievert PM, Bergdoll MS, Novick RP. 1983. The toxic shock syndrome exotoxin structural gene is not detectably transmitted by a prophage. Nature 305:709–712. https://doi.org/10.1038/305709a0.
95. Rosenstein R, Nerz C, Biswas L, Resch A, Raddatz G, Schuster SC, Götz F. 2009. Genome analysis of the meat starter culture bacterium *Staphylococcus carnosus* TM300. Appl Environ Microbiol 75:811–822. https://doi.org/10.1128/AEM.01982-08.
96. Swoboda JG, Meredith TC, Campbell J, Brown S, Suzuki T, Bollenbach T, Malhowski AJ, Kishony R, Gilmore MS, Walker S. 2009. Discovery of a small molecule that blocks wall teichoic acid biosynthesis in *Staphylococcus aureus*. ACS Chem Biol 4:875–883. https://doi.org/10.1021/cb900151k.
97. Sievers F, Wilm A, Dineen D, Gibson TJ, Karplus K, Li W, Lopez R, McWilliam H, Remmert M, Soding J, Thompson JD, Higgins DG. 2011. Fast, scalable generation of high-quality protein multiple sequence alignments using Clustal Omega. Mol Syst Biol 7:539. https://doi.org/10.1038/msb.2011.75.
98. Sullivan MJ, Petty NK, Beatson SA. 2011. Easyfig: a genome comparison visualizer. Bioinformatics 27:1009–1010. https://doi.org/10.1093/bioinformatics/btr039.